bioRxiv preprint doi: https://doi.org/10.1101/041533; this version posted October 13, 2017. The copyright holder for this preprint (which was not certified by peer review) is the author/funder, who has granted bioRxiv a license to display the preprint in perpetuity. It is made available under aCC-BY-NC 4.0 International license.

Increased pollination specialization did not increase corolla shape constraints in Antillean plants

Simon Joly[1,2,*], François Lambert[2], Hermine Alexandre[2], Julien Clavel[3], Étienne Léveillé-Bourret[2,**], and John L. Clark[4]

[1] *Montreal Botanical Garden, Montréal, Canada*

[2] *Institut de recherche en biologie végétale, Département de sciences biologiques, Université de Montréal, Montréal, Canada*

[3] *Institut de biologie, École Normale Supérieure, Paris, France*

[4] *Department of Biological Sciences, The University of Alabama, Tuscaloosa, USA*

[*] *To whom correspondance should be addressed: Institut de recherche en biologie végétale, 4101 Sherbrooke East, Montréal (QC) H1X 2B2, Canada; +1 514.872.0344; joly.simon@gmail.com.*

[**] *Present address: Department of Biology, University of Ottawa, Ottawa, Canada*

bioRxiv preprint doi: https://doi.org/10.1101/041533; this version posted October 13, 2017. The copyright holder for this preprint (which was not certified by peer review) is the author/funder, who has granted bioRxiv a license to display the preprint in perpetuity. It is made available under aCC-BY-NC 4.0 International license.

Abstract

Flowers show important structural variation as reproductive organs but the evolutionary forces underlying this diversity are still poorly understood. In animal-pollinated species, flower shape is strongly fashioned by selection imposed by pollinators, which is expected to vary according to guilds of effective pollinators. Using the Antillean subtribe Gesneriinae (Gesneriaceae), we tested the hypothesis that pollination specialists pollinated by one functional type of pollinator have maintained more similar corolla shapes through time due to stronger selection constraints compared to species with more generalist pollination strategies. Using geometric morphometrics and evolutionary models, we showed that the corolla of hummingbird specialists, bat specialists, and species with a mixed-pollination strategy (pollinated by hummingbirds and bats; thus a more generalist strategy) have distinct shapes and that these shapes have evolved under evolutionary constraints. However, we did not find support for smaller disparity in corolla shape for hummingbird specialists compared to more generalist species. This could be because the corolla shape of more generalist species in subtribe Gesneriinae, which has evolved multiple times, is finely adapted to be effectively pollinated by both bats and hummingbirds. These results suggest that pollination generalization is not necessarily associated with relaxed selection constraints.

Key-words: Pollination syndromes, specialists-generalists, geometric morphometrics, phylogenetic comparative methods, Ornstein-Uhlenbeck (OU) models, stabilizing selection.

bioRxiv preprint doi: https://doi.org/10.1101/041533; this version posted October 13, 2017. The copyright holder for this preprint (which was not certified by peer review) is the author/funder, who has granted bioRxiv a license to display the preprint in perpetuity. It is made available under aCC-BY-NC 4.0 International license.

Introduction

The variation of flower shapes and structures we observe in nature is a constant reminder of the power of natural selection. This diversity is often attributed to zoophilous pollination, which has been associated with increased diversification in angiosperms (Stebbins, 1970; Crepet, 1984; Johnson, 2010; van der Niet and Johnson, 2012). Indeed, pollinator-driven selection pressure has been associated with species diversification (Whittall and Hodges, 2007) and frequent pollinator shifts often correlate with increased species diversification rates (e.g., Valente et al., 2012; Forest et al., 2014; Breitkopf et al., 2015). Yet, despite the numerous studies on pollination-driven selection at the population level (reviewed below), on the dissection of the genetic basis of several floral transitions between species pollinated by different pollinators (reviewed in: Galliot et al., 2006; Yuan et al., 2013) and of phylogenetic investigations of pollination systems at macroevolutionary levels (e.g., Perret et al., 2007; Smith, 2010), there is still a gap in our understanding on how the microevolutionary forces operating at the population level shape the macroevolutionary patterns we observe (Waser, 1998).

Selection can affect flower morphology differently when a population is adapting to a novel pollinator guild (transition phase) compared to when it is under the influence of a relatively constant pollinator guild (stasis phase). The transition phase is expected to involve strong directional selection until the population has a phenotype close to the optimum for the new pollinators (Lande, 1976). Studies on pollinator-mediated selection have found evidence for strong directional selection for flower shape in the transition phase (Galen, 1989), while others have shown that pollinators can drive flower colour transitions in populations (Waser and Price, 1981; Stanton et al., 1986). Although not a direct measurement of selection, the numerous studies reporting geographically structured flower variation associated with variation in pollinator guilds further support these findings (e.g., Gómez and Perfectti, 2010; Newman et al., 2014; Niet et al., 2014; Martén-Rodríguez et al., 2011), especially when reciprocal transplant experiments confirmed these patterns (Newman et al., 2012; Boberg et al., 2014; Sun et al., 2014).

For populations in stasis phase, that is with a relatively constant selection pressure from a stable pollinator guild, the floral traits are expected to be under stabilizing selection around

bioRxiv preprint doi: https://doi.org/10.1101/041533; this version posted October 13, 2017. The copyright holder for this preprint (which was not certified by peer review) is the author/funder, who has granted bioRxiv a license to display the preprint in perpetuity. It is made available under aCC-BY-NC 4.0 International license.

optimal trait values. The mean phenotype of a population evolving under stabilizing selection is affected by both selection and drift, with selection pulling the mean phenotype towards the fitness optimum and drift due to finite population sizes moving it in random directions (Lande, 1976, 1979). Although stabilizing selection on floral traits have sometimes been observed in pollinator-mediated selection studies (Sahli and Conner, 2011; Conner et al., 2003), most studies failed to find such evidence (Campbell et al., 1991; O'Connell and Johnston, 1998; Maad, 2000). This might be because these phases are not so stable and that these studies are typically performed on a yearly basis. Indeed, studies have shown that selection on floral traits can vary from year to year in populations (Campbell, 1989; Campbell et al., 1991) due to temporal variation in pollinator abundance or environmental conditions. Nevertheless, there is considerable evidence that traits involved in the mechanical fit between the flower and the pollinators are under long-term stabilizing selection pressure as they show less variation in populations than other traits (Muchhala, 2006; Cresswell, 1998). Interestingly, these observations suggest that evidence for such stabilizing selection might be better studied over many generations, or even at macroevolutionary scales, than for a single generation (see also Haller and Hendry, 2014).

The intensity of constraints during the stasis phase is also expected to vary according to the level of pollination generalization of the species of interest. If the flower shape of specialist flowers should show evidence of stabilizing selection around an optimal shape adapted to its pollinator, the expectations are less clear for flowers of generalist species that possess pollinators that are functionally different for the plant (Aigner, 2001, 2006; Sahli and Conner, 2011). In general, unless the different functional pollinators all select for a common shape (common peak model: Sahli and Conner, 2011), generalists effectively pollinated by more than one functional type of pollinators are expected to be under weaker selection constraints than specialists (Johnson and Steiner, 2000). These predictions do not seem to have been tested thoroughly but are important to understand how and why flowers diversify under the selection of animal pollinators (Johnson, 2010).

In this study, we used a macroevolutionary approach to test whether increased specialisation in pollination strategies is associated with reduced corolla shape diversification (disparity) caused by stronger long-term selective constraints in species of the subtribe Gesneriinae

bioRxiv preprint doi: https://doi.org/10.1101/041533; this version posted October 13, 2017. The copyright holder for this preprint (which was not certified by peer review) is the author/funder, who has granted bioRxiv a license to display the preprint in perpetuity. It is made available under aCC-BY-NC 4.0 International license.

of the Gesneriaceae family in the Caribbean islands. The recent development of powerful phylogenetic comparative methods allows the estimation of historic selective constraints on large groups of species (e.g., Hansen and Martins, 1996; Beaulieu et al., 2012; Butler and King, 2004) and thus testing specific hypotheses regarding the role of pollinators on floral trait evolution (e.g., Gómez et al., 2015). Unlike many investigations performed at the population level, such approaches aim at measuring selective constraints in terms of selective optima or in the rate at which disparity accrues over macroevolutionary scales and, as such, should be informative to understand the forces that have been determinant in modelling the morphology of large groups of species.

The subtribe Gesneriinae represents an ideal group to test this hypothesis. This diverse group in terms of floral morphologies is almost completely endemic to the Antilles and diversified into approximately 81 species (Skog, 2012) during the last 10 millions years (Roalson et al., 2008; Roalson and Roberts, 2016). The group has been the subject of several pollination studies that classified the species into different pollination syndromes that vary in their degree of ecological specialization (Martén-Rodríguez and Fenster, 2008; Martén-Rodríguez et al., 2009, 2010, 2015). There exists several definitions of pollination specialization/generalization, but globally plants pollinated by more species are considered more generalist (see papers in Waser and Ollerton, 2006), although information on the relative abundance (Medan et al., 2006) and functional diversity of pollinators (Johnson and Steiner, 2000; Fenster et al., 2004; Gómez and Zamora, 2006) should ideally taken into account. Here, we follow Fleming and Muchhala (2008) and measure ecological specialization with respect to the number of effective functional pollinator groups, with species pollinated by more functional pollinator groups being more generalists.

Specialist pollination strategies in Gesneriinae include hummingbird pollination, bat pollination, moth pollination and bee pollination (Fig. 1). Species with these strategies are pollinated by a single functional type (or guild) of pollinator and most often by a single species (Martén-Rodríguez and Fenster, 2008; Martén-Rodríguez et al., 2009, 2010, 2015). A fifth pollination strategy is considered more generalist as it is effectively pollinated in similar proportion by hummingbirds and bats (Martén-Rodríguez et al., 2009), two pollinators belonging to different functional groups that have different plant (growth form) and

bioRxiv preprint doi: https://doi.org/10.1101/041533; this version posted October 13, 2017. The copyright holder for this preprint (which was not certified by peer review) is the author/funder, who has granted bioRxiv a license to display the preprint in perpetuity. It is made available under aCC-BY-NC 4.0 International license.

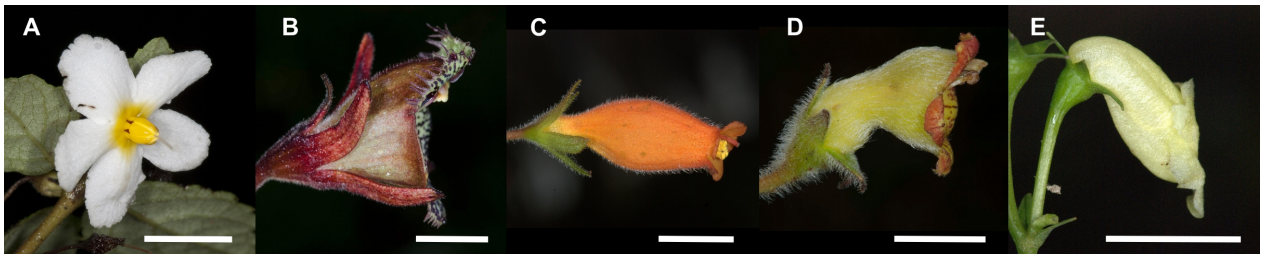

Figure 1: Gesneriinae flowers showing the different pollination strategies discussed in the study: (A) bee pollination (*Bellonia spinosa*, voucher: XXX); (B) bat pollination (*Gesneria fruticosa*, voucher: XXX); C) hummingbird pollination (*Rhytidophyllum rupincola*, voucher: XXX); D) mixed-pollination (*Rhytidophyllum auriculatum*, voucher: XXX); E) moth pollination (*Gesneria humilis*, voucher: XXX). The bar indicates 1 cm. Photographs by XXX.

floral (nectar, shape, colour) preferences (Baker, 1961; Faegri and van der Pijl, 1979; Flemming et al., 2005). Although there exists many examples of more generalist species, these species are nevertheless ecologically more generalized than species pollinated by a single functional group of pollinators because they rely on more diversified resources (Gómez and Zamora, 2006). To avoid confusion with super-generalist species, we will use the term mixed-pollination strategy to refer to them in this study. Species of the Gesneriinae are sometimes visited by insects, but these always have marginal importance (Martén-Rodríguez and Fenster, 2008; Martén-Rodríguez et al., 2009, 2015) except for the insect pollination syndromes. A phylogenetic study of the group suggested multiple origins of most pollination strategies (Martén-Rodríguez et al., 2010), making it a perfect group to study selective forces acting on each one. In this study, we augmented previous phylogenetic hypotheses of the group by adding more species and genetic markers and we used geometric morphometrics of corolla shape and evolutionary models to test that (1) corolla shape evolution in the group supports distinct pollination syndromes, (2) corolla shape evolution is characterized by long-term constraints, and that (3) the corolla shape of pollination specialists show reduced disparity compared to the mixed-pollination species.

bioRxiv preprint doi: https://doi.org/10.1101/041533; this version posted October 13, 2017. The copyright holder for this preprint (which was not certified by peer review) is the author/funder, who has granted bioRxiv a license to display the preprint in perpetuity. It is made available under aCC-BY-NC 4.0 International license.

Material and Methods

Floral morphology and pollination strategies

We took and collected photographs of 137 flowers in anthesis (137 distinct individuals, all from different localities) in longitudinal view, from 50 species (supplementary Table S1, S2; picture thumbnails are available as supplementary material) for a mean of 2.8 individuals per species (sd. dev. = 2.4). Most of these were taken in the wild, but a few specimens came from botanical gardens. We also took three pictures of the same flower (releasing and grabbing the pedicel between pictures) for four species at the Montreal Botanical Garden to quantify the error involved in hand-photographing the specimens as this is how most specimens were photographed.

Pollinator information was obtained from the literature (Martén-Rodríguez and Fenster, 2008; Martén-Rodríguez et al., 2009, 2010, 2015). Pollination strategy of species without field observation were inferred following the conclusions of Martén-Rodríguez et al. (2009). Briefly, hummingbird specialists have straight tubular corollas with bright colours and diurnal anthesis, bat specialists have green or white campanulate (bell-shaped) corollas with nocturnal anthesis and exserted anthers, and species with a mixed-pollination strategy are intermediate with subcampanulate corollas (bell-shaped with a basal constriction) showing various colours with frequent coloured spots, and diurnal as well as nocturnal anther dehiscence and nectar production (Martén-Rodríguez et al., 2009, Fig. 1). So far, only one moth pollinated species has been observed and it has a pale pouched corolla (Fig. 1). All analyses were performed (1) using only species with confirmed pollinator information and (2) also adding species with inferred strategies. We followed the taxonomy of Skog (2012) except for recent modifications in the *Gesneria viridiflora* complex (unpublished data).

Molecular methods

A total of 94 specimens were included in the phylogenetic analyses (supplementary Table S3). *Koehleria* sp. 'Trinidad' (tribe Gesnerieae) and *Henckelia malayana* (tribe Trichosporeae) were included as outgroups. DNA was extracted using the plant DNA extraction kits from

bioRxiv preprint doi: https://doi.org/10.1101/041533; this version posted October 13, 2017. The copyright holder for this preprint (which was not certified by peer review) is the author/funder, who has granted bioRxiv a license to display the preprint in perpetuity. It is made available under aCC-BY-NC 4.0 International license.

QIAGEN (Toronto, Ontario) or BioBasics (Markham, Ontario). Five nuclear genes were amplified and sequenced: *CYCLOIDEA*, *CHI*, *UF3GT*, *F3H*, *GAPDH*. The first four are unlinked (unpublished linkage map), whereas no data is available for *GAPDH*. Primer sequences and PCR conditions can be found in supplementary Table S4. Sequencing reactions were performed by the Genome Quebec Innovation Centre and run on a 3730xl DNA Analyzer (Applied Biosystems). Sequences from both primers were assembled into contigs and corrected manually in Geneious vers. 1.8. DNA sequences generated for this study were augmented with previously published sequences (supplementary Table S3).

Phylogenetic analyses

Gene sequences were aligned using MAFFT (Katoh and Standley, 2013). Ambiguous alignment sections in intron regions of *CHI* and *GAPDH* were removed using gblocks (Castresana, 2000) with the default settings. Alignments were verified by eye and no obviously misaligned region remained after treatment with gblocks. Substitution models were selected by Akaike Information Criterion (AIC) with jModeltest 2 (Darriba et al., 2012) using an optimized maximum likelihood tree. A species tree was reconstructed using *BEAST in BEAST ver. 1.8.2 (Drummond et al., 2012). A Yule prior was chosen for the tree, a lognormal relaxed molecular clock for gene trees, and a gamma (2,1) prior for gene rates. Other parameters were left to the default settings. Three independent Markov Chain Monte Carlo (MCMC) analyses of 1×10^8 generations were performed, sampling trees and parameters every 10,000 generations. Convergence of the runs was reached for parameter values, tree topology and clade posterior probabilities. The first 2×10^7 generations were discarded as burnin and the remaining trees were combined for the analyses. The maximum clade credibility tree with median node heights was used for graphical representation.

Geometric morphometric analyses

Six landmarks and 26 semi-landmarks were positioned on photographs using `tpsDig2` (Rohlf, 2010). Two landmarks were positioned at the base of the corolla, two at the tips of the petal lobes, and two at the base of the petal lobes, which generally corresponds to the corolla tube

bioRxiv preprint doi: https://doi.org/10.1101/041533; this version posted October 13, 2017. The copyright holder for this preprint (which was not certified by peer review) is the author/funder, who has granted bioRxiv a license to display the preprint in perpetuity. It is made available under aCC-BY-NC 4.0 International license.

opening. The semi-landmarks were then positioned at equal distance along the curve of the corolla (13 on each side) between the landmarks at the base of the corolla and at the base of the petal lobes. The sepals were present on most of the pictures. The landmark data was imported in `R` (R core team, 2014) where it was transformed by generalized Procrustes analysis using the `geomorph R` package (Adams and Otárola-Castillo, 2013). The semi-landmarks on curves were slid along their tangent directions during the superimposition by minimizing the Procrustes distance between the reference and target specimen (Bookstein, 1997). Size was not considered in the analyses because we were interested in shape and because a scale was not available for all specimens. Because the actinomorphic flowers of bee pollinated species (*Bellonia ssp.*) do not allow homologous placement of landmarks, these were dropped from the morphometric analyses.

Landmarks were positioned twice for each photograph and a Procrustes ANOVA quantified the variance explained by these technical replicates, which were combined for the remaining analyses. We also used a Procrustes ANOVA to quantify the variation among the replicated photographs of the same flowers; these replicates were not included in the final analyses. The Procrustes aligned specimens were projected into the tangent space, hereafter the morphospace, using Principal Component Analysis (PCA) of the covariance matrix using the `prcomp` function in `R`.

To characterize the total morphological variation for each pollination strategy, we estimated the distance of the mean corolla shape of each species to the pollinator strategy centroid in multivariate space and tested if these distances were different for the different pollination strategies using the `betadisper` function of the `vegan` package in `R` (Oksanen et al., 2017). The differences were tested by ANOVA. We also partitioned the variation into intraspecific and interspecific components for each pollination strategy using Procrustes ANOVA, reporting adjusted R^2 values.

Morphological integration (Klingenberg, 2013) was quantified using the variance of the eigenvalues of a PCA on the covariance matrix (Pavlicev et al., 2009; Klingenberg, 2013), scaling the eigenvalues by the total variance of the sample to get an index independent of the total sample variation (Young, 2006). This was estimated on all individuals for the hummingbird and mixed-pollination species. Bat specialists were omitted from this analysis

bioRxiv preprint doi: https://doi.org/10.1101/041533; this version posted October 13, 2017. The copyright holder for this preprint (which was not certified by peer review) is the author/funder, who has granted bioRxiv a license to display the preprint in perpetuity. It is made available under aCC-BY-NC 4.0 International license.

because there were too few species to give a result comparable to the other pollination strategies.

Ancestral states reconstruction

Ancestral state reconstruction was performed to estimate the probability of all pollination strategy states for all nodes of the phylogeny. The best transition model was first selected by second order AIC (AICc) with the `geiger` `R` package (Harmon et al., 2008). Eight models selected based on biological relevance were compared. The Equal Rate (ER), Symmetric (SYM) and All Rates Different (ARD) were tested with modified versions that give a single rate to and from the moth and bee states (ER.2, SYM.2, and ARD.2). In addition, a 4-rate model was tested where rates differed according to the actual state and a single rate to and from the bee and moth states, and finally a 3-rate model with one rate for transitions from and to bee and moth states, one from hummingbirds to bats or mixed-pollination, and a third from bat or mixed-pollination to all states except bee or moth. Using the best model, the joint ancestral state probabilities were estimated using stochastic character mapping (Huelsenbeck et al., 2003) on the maximum clade credibility tree with 2000 simulated character histories. When estimating ancestral states with only species with confirmed pollinators, the other species were given equal prior probabilities in the simulations. To estimate the number of transitions between states while accounting for phylogenetic uncertainty, 500 character histories were simulated on 2000 species trees randomly sampled from the posterior distribution from the species tree search using the `phytools` `R` package. The median number of transitions between all states from all simulated character histories were reported as well as 95% credible intervals.

Evolutionary constraints on flower shape

Given the nature of the hypotheses tested, two types of evolutionary models based on the Brownian motion (BM) and the Ornstein-Uhlenbeck (OU) stochastic processes were considered. BM models the accumulation of independent and infinitesimal stochastic phenotypic changes (controlled by the drift rate parameter σ^2) along the branches of a phylogeny; it can

bioRxiv preprint doi: https://doi.org/10.1101/041533; this version posted October 13, 2017. The copyright holder for this preprint (which was not certified by peer review) is the author/funder, who has granted bioRxiv a license to display the preprint in perpetuity. It is made available under aCC-BY-NC 4.0 International license.

approximate various scenarios of phenotypic evolution such as drift, fluctuating directional selection or punctuated change (Felsenstein, 1985; Hansen and Martins, 1996; O'Meara et al., 2006). In contrast, the OU process models selection toward a common optimal trait value (Felsenstein, 1988; Hansen and Martins, 1996) and adds to the BM model a selection parameter α that determines the strength of selection towards an optimal trait θ (details on the models can be found in Hansen and Martins, 1996; Butler and King, 2004; Beaulieu et al., 2012). When the strength of selection is null ($\alpha = 0$), the OU process reduces to BM. These models can be made more complex, for instance by allowing parameters to vary in different parts of the tree (selective regimes - e.g., Butler and King, 2004; O'Meara et al., 2006; Beaulieu et al., 2012) and are therefore useful for characterizing the evolutionary constraints of the pollination strategies.

Generalist pollination is hypothesized to promote phenotypic diversification (disparity) of corolla shape because it is thought to be under weaker selection (Johnson and Steiner, 2000), but also because of the spatio-temporal variation in pollinator abundance that could result in fluctuating selection pressures (Herrera, 1988) or in a variety of species- or population-specific adaptive peaks (see Discussion). As such, mixed-pollination species are expected to best fit a BM process. In contrast, due to their adaptation to a single functional pollinator, pollination specialists are expected to show smaller variation around a better defined shape optimum and thus fit an OU process. However, BM and OU processes can be difficult to distinguish, and an OU process can best fit the data for other reasons such as measurement error (Silvestro et al., 2015), bounded trait variation (Boucher and Démery, 2016) or small sample sizes (Cooper et al., 2016). In contrast, OU models are less likely to be selected when analyzing the primary axes of variation from a PCA (Uyeda et al., 2015). Therefore, prediction of higher phenotypic disparity is often better assessed through evaluation of parameters estimated under OU or BM for species pollinated by different functional groups of pollinators. For instance, with the BM process, the drift rate (σ^2) describes the accumulation of phenotypic variance over the tree and is therefore tightly related to phenotypic disparity (O'Meara et al., 2006; Thomas et al., 2006; Price et al., 2013). Following our hypothesis of lower phenotypic disparity for pollination specialists, we predict they should have a smaller σ^2 compared to mixed-pollination species. Similarly, under an OU model, the stationary variance around an optimum, expressed as

bioRxiv preprint doi: https://doi.org/10.1101/041533; this version posted October 13, 2017. The copyright holder for this preprint (which was not certified by peer review) is the author/funder, who has granted bioRxiv a license to display the preprint in perpetuity. It is made available under aCC-BY-NC 4.0 International license.

$\sigma^2/2\alpha$ for the univariate case, is also tightly related to phenotypic disparity. We thus expect pollination specialists to be associated with stronger corolla shape constraints (i.e., higher α values) and smaller stationary variances compared to mixed-pollination species in models where either α or σ^2 vary between strategies (see below). Finally, we expect phenotypic evolutionary correlations between traits inferred from multivariate comparative models to be higher in pollination specialists (i.e., higher phenotypic integration, see for instance Revell and Collar, 2009).

We evaluated and compared the model fit and parameter estimates with the predictions of our hypotheses using univariate and multivariate models because they allow investigating different aspects of the data. Univariate models allowed us to fit a greater range of evolutionary models that are not yet implemented in multivariate approaches and allow investigating if different shape components evolved under similar constraints. In contrast, multivariate models allow to fit an evolutionary model on several shape components at once and also allow to investigate patterns of evolutionary correlation among traits for the different pollination strategies; that is, studying phenotypic integration in an evolutionary context. For univariate models, we fitted BM models with one drift rate for the whole tree (BM1) and with one rate per regime (BMV), but also versions that allow different ancestral states for the different regimes (O'Meara et al., 2006; Thomas et al., 2009); model BM1m has distinct trait means per regime but a single drift rate across the tree, while BMVm has distinct means and drift rates for each regime. We also fitted different variants of the OU models (Beaulieu et al., 2012): with a single optimum θ (OU1), with different optima for lineages with different pollination strategies (OUM), different θ and selective strength α (OUMA), different θ and rates of stochastic motion σ^2 (OUMV), or different θ, α and σ^2 (model OUMVA) for the different pollination strategies. We also considered ecological release models, in which one regime on the tree is evolving under BM and the other under an OU process, either with a shared drift rate σ^2 (OUBM and BMOU) or with their own drift rates (models OUBMi and BMOUi) which are sometimes called ecological release and radiate models (see Slater, 2013). The model OUBM considers hummingbird specialists to be evolving under an OU model whereas the mixed-pollination species are evolving under a BM model, and vice versa. Several multivariate models were also considered: BM1, BMV, BM1m, BMVm, OU1, OUM,

bioRxiv preprint doi: https://doi.org/10.1101/041533; this version posted October 13, 2017. The copyright holder for this preprint (which was not certified by peer review) is the author/funder, who has granted bioRxiv a license to display the preprint in perpetuity. It is made available under aCC-BY-NC 4.0 International license.

OUBM, BMOU, OUBMi, and BMOUi. The multivariate OU models allowing different contraints on different regimes (OUMA, OUMV, OUMVA) are not implemented yet and thus we can not estimate regime specific evolutionary covariance (or correlation) matrices. However, we expect such models to be over-parameterized with respect to the number of species considered in our study.

In the remaining, we therefore consider the comparison of phenotypic evolutionary correlations obtained from the σ^2 correlation matrices of the multivariate BM models only. Yet, focussing on the interpretation of parameters obtained under the BM processes can be misleading if BM is a poor descriptor of the phenotypic evolution (see for instance Price et al., 2013). To make sure this did not affect our estimates, we simulated datasets using a OUM model on 100 trees randomly selected from the posterior distribution using the parameters estimated from the observed data. We then fitted these simulated data with the BMVm model to obtain σ^2 correlation matrices that were compared with the original σ^2 correlation matrices.

The models were fitted for the first three principal components of the morphospace using the `R` packages `mvMORPH` (Clavel et al., 2015) and `OUwie` (Beaulieu et al., 2012). The models were fitted on a sample of 1000 trees from the posterior distribution of species trees on which the character history was inferred by one instance of stochastic mapping (Huelsenbeck et al., 2003) using maximum likelihood in the `phytools R` package (Revell, 2012). This accounts for phylogenetic uncertainty and the stochasticity of the character state reconstructions (Revell, 2013). All the trees were re-scaled to unit height. Intraspecific variation was taken into account by using the sampling variance (the squared standard error) of species as measurement error in model fitting; species without biological replicates were given the mean squared standard error of species with the same pollination strategy. The models were compared using $AICc$ weights that can be roughly considered as the relative weight of evidence in favour of a model given a set of models (Burnham and Anderson, 2002). The analyses were performed with inferred pollination strategies as well as with species with confirmed pollination strategies only. Note that because there were few confirmed bat pollinated species and a single moth pollinated species, species with these pollination strategies were excluded from the analyses. However, the inclusion of bat pollinated species in the univariate models

bioRxiv preprint doi: https://doi.org/10.1101/041533; this version posted October 13, 2017. The copyright holder for this preprint (which was not certified by peer review) is the author/funder, who has granted bioRxiv a license to display the preprint in perpetuity. It is made available under aCC-BY-NC 4.0 International license.

did not affect the conclusions (data not shown). The data and scripts used to replicate all analyses are available as supplementary information.

Results

Phylogeny

The species phylogeny showed that the bee pollinated genus *Bellonia* is sister to the rest of the subtribe, and the subtribe (*Bellonia* + *Gesneria* + *Rhytidophyllum*) received a posterior probability of 1 (not shown). *Rhytidophyllum* and *Gesneria* were found to form distinct clades, although *Gesneria* received weaker support (Fig. 2). This reinforces the distinction between these two genera, which has been debated over the years. There is one exception, *Rhytidophyllum bicolor*, which is included for the first time in a molecular phylogeny and that falls within *Gesneria*. The taxonomic name of this species will have to be reconsidered. Several branches show strong clade posterior probabilities, but some had less support due to lack of phylogenetic signal or conflict between gene trees, indicating the importance of incorporating phylogenetic uncertainty in the following analyses.

The best character evolutionary model (smallest $AICc$) was the 3 rates model with one rate for transitions from and to the bee and moth states, one from hummingbirds to bats or mixed-pollination, and a third from bat or mixed-pollination to all states except bee and moth. Ancestral state reconstruction (Fig. 2) suggests that the hummingbird pollination is the most likely ancestral state for the *Gesneria* clade, although it is only slightly more likely than an ancestral mixed-pollination strategy. In contrast, the mixed-pollination strategy is the most probable ancestral state for the *Rhytidophyllum* clade. A hummingbird pollinated ancestor for the subtribe is more probable, but only very slightly. This reflects the difficulty in estimating the ancestral states for nodes near the root of a phylogeny (Gascuel and Steel, 2014). The ancestral state reconstruction with the inferred pollination strategies (Fig. S1) were highly similar to those of Fig. 2.

Estimation of the number of transitions supports several transitions between the bat, the mixed-pollination and the hummingbird strategies (Table 1). The number of transition from mixed-pollination to hummingbird and from mixed-pollination to bat was slightly higher than

bioRxiv preprint doi: https://doi.org/10.1101/041533; this version posted October 13, 2017. The copyright holder for this preprint (which was not certified by peer review) is the author/funder, who has granted bioRxiv a license to display the preprint in perpetuity. It is made available under aCC-BY-NC 4.0 International license.

Table 1: Number of transitions between the different pollination strategies according to stochastic mapping. The median values obtained from the character simulations over the posterior distribution of species tree is reported as well as 95% credible intervals. Ancestral states are in rows.

	bat	bee	hummingbird	mixed-pollination	moth
bat	–	0.30 [0.22, 0.37]	3.31 [2.79, 3.88]	3.52 [3.10, 3.91]	0.26 [0.17, 0.31]
bee	0.07 [0.02, 0.12]	–	0.07 [0.03, 0.11]	0.08 [0.03, 0.14]	0.04 [0.03, 0.07]
hummingbird	2.61 [2.16, 3.03]	0.61 [0.52, 0.71]	–	2.52 [2.10, 2.89]	0.84 [0.71, 0.98]
mixed-pollination	4.30 [3.68, 4.77]	0.36 [0.29, 0.43]	4.87 [4.14, 5.51]	–	0.31 [0.21, 0.37]
moth	0.04 [0.02, 0.06]	0.08 [0.04, 0.11]	0.05 [0.03, 0.08]	0.04 [0.02, 0.07]	–

from bat to mixed-pollination and bat to hummingbird, which was also slightly higher than the number of transitions from hummingbird to bats and hummingbird to mixed-pollination (Table 1). However, because the confidence intervals largely overlap, we can conclude that the number of transitions between these three main pollination strategies are not significantly different. The results were almost identical when analyses were performed with inferred pollination strategies (Supplementary Table S5). These estimates are similar to those of Martén-Rodríguez et al. (2010), although they found fewer reversals to hummingbirds in their study. Overall, these results confirm multiple evolutionary origins for all pollination strategies except for the bee and moth (95 % CI always > 2; Table 1).

Corolla shape

We found only 0.15% of variation between independent pictures of the same flower in the replication experiment, which is lower than the variation involved in the landmark positioning (0.81%). Therefore, we conclude that the error included in the data by the picture acquisition was minimal. Similarly, because the technical replicates accounted for only 0.56% of the total variance in the final dataset, the mean shape between replicates was used for the remaining analyses.

The morphospace explained 79% of the total shape variance in the first three axes. The first principal component (PC) represents 53.6% of the variance and is characterized by campanulate vs. tubular corollas (Fig. 3A), broadly differentiating hummingbird specialists from the other species. This concurs with a previous study that showed that this was indeed the main characteristic differentiating the hummingbird pollination strategy from the bat and the mixed-pollination strategies (Martén-Rodríguez et al., 2009). PC2 explains 20.6% of the variance and is characterized by corolla curvature and distinguished the moth pollinated

bioRxiv preprint doi: https://doi.org/10.1101/041533; this version posted October 13, 2017. The copyright holder for this preprint (which was not certified by peer review) is the author/funder, who has granted bioRxiv a license to display the preprint in perpetuity. It is made available under aCC-BY-NC 4.0 International license.

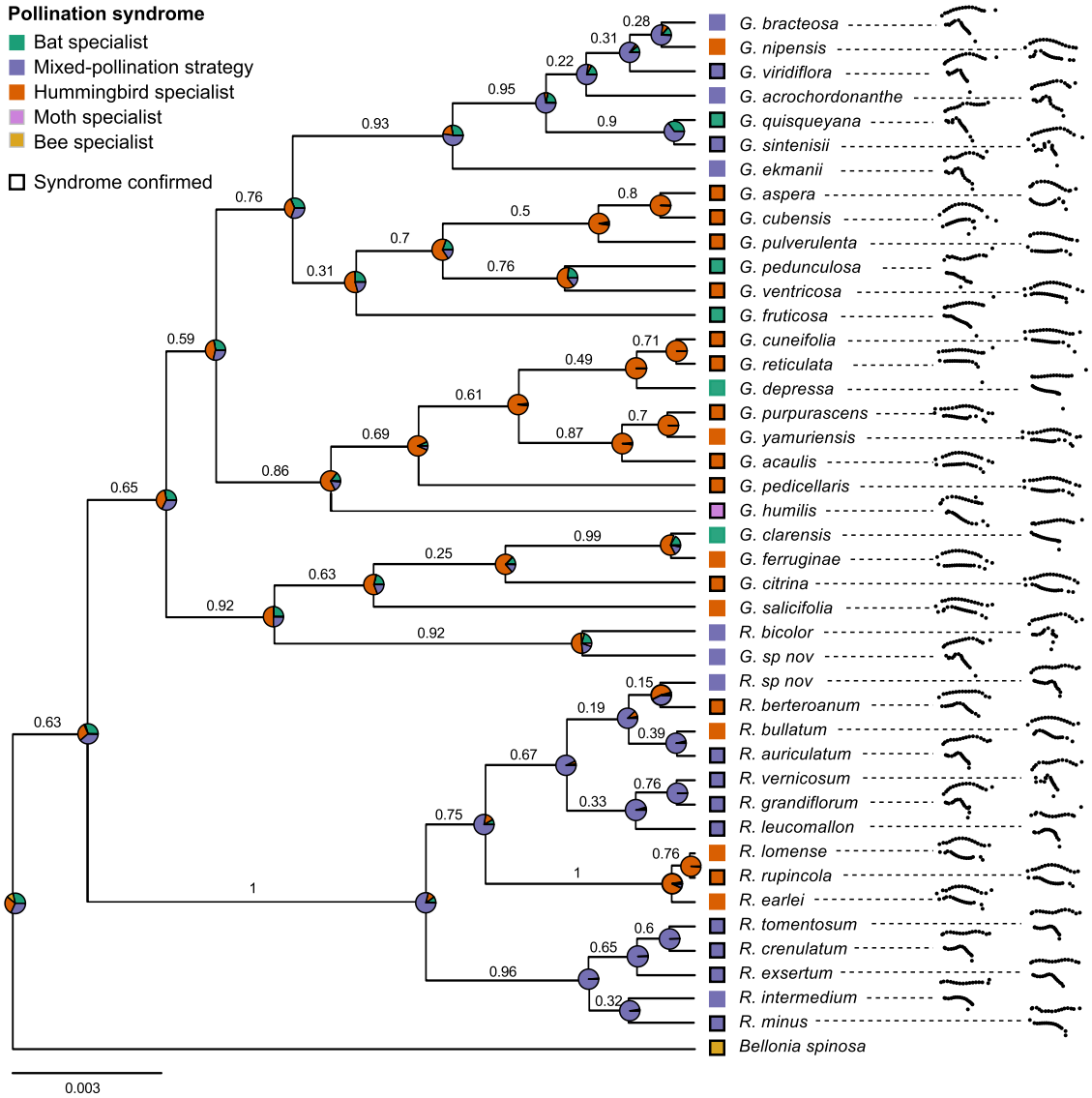

Figure 2: Species phylogeny showing mean corolla shapes (after Procrustes analysis). Pollination strategies are shown with those that have been confirmed indicated by a black contour. Pie charts represent the joint probability of each state at nodes as estimated by stochastic mapping from only species with confirmed pollinators. Clade posterior probabilities are shown above branches. Outgroup taxa are not shown.

bioRxiv preprint doi: https://doi.org/10.1101/041533; this version posted October 13, 2017. The copyright holder for this preprint (which was not certified by peer review) is the author/funder, who has granted bioRxiv a license to display the preprint in perpetuity. It is made available under aCC-BY-NC 4.0 International license.

G. humilis. The bat and the mixed-pollination strategies could not be differentiated with this PCA, but a second PCA that excluded moth and hummingbird pollinated species (both confirmed and inferred) found that the bat and mixed-pollination strategies were separated along PC3 that is characterized by a basal constriction in the corolla (Fig. 3B), a character known to distinguish bat pollinated species (that generally lack the constriction) from species with a mixed-pollination strategy (Martén-Rodríguez et al., 2009). The single bat pollinated species that groups with mixed-pollination species on this axis is *Gesneria quisqueyana* (see interactive supplementary figures for information on the individual and species positioning in the PCAs), which, in contrast to other bat pollinated species in the group, excludes hummingbirds during the day by actively closing its flowers (Martén-Rodríguez et al., 2009).

Variation partitioning

The pollination strategies did not have a significantly different corolla variation among species (ANOVA: F = 1.92, df = 2, $p = 0.1654$). The partitioning of the shape variance for the different pollination strategies showed that the proportion of variance explained among species corresponded to 81.4% ($p < 0.001$) for hummingbird pollinated species, 91.3% ($p = 0.22$) for bat pollinated species and 50.4% ($p < 0.001$) for mixed-pollination species. The result of the variance partitioning for the bat pollinated species should be interpreted with caution because there was only three species with less than two replicated individuals on average within species for this syndrome.

Morphological integration

Flower components are generally well integrated as they develop, function and evolve jointly (Ashman and Majetic, 2006), a concept called morphological integration (reviewed in Klingenberg, 2013). A large morphological integration index supports important integration because morphological variation is concentrated in few principal components. The results showed that species with a mixed-pollination strategy had a slightly greater morphological integration (0.0069) than hummingbird pollinated species (0.0050).

bioRxiv preprint doi: https://doi.org/10.1101/041533; this version posted October 13, 2017. The copyright holder for this preprint (which was not certified by peer review) is the author/funder, who has granted bioRxiv a license to display the preprint in perpetuity. It is made available under aCC-BY-NC 4.0 International license.

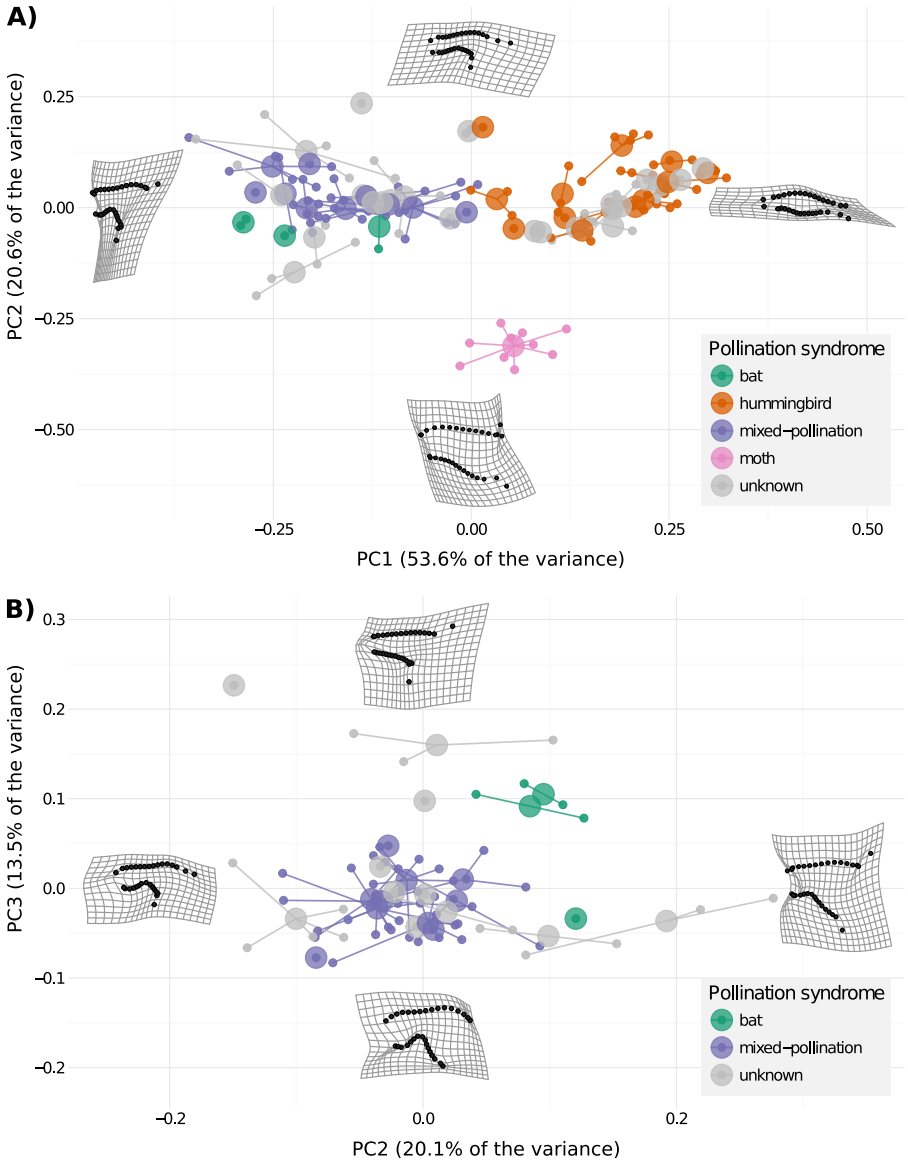

Figure 3: Principal component analyses showing the corolla shape morphospace for (A) all species and (B) species excluding hummingbird (both confirmed and inferred) and moth pollinated species. The large dots on the plot represent the species means, which are connected by a line to the floral shapes of the individuals belonging to the species (small dots). Thin-plate spline deformation grids show corolla shape variation along the principal components (plus or minus 2 standard deviation from the mean shape). *Bellonia spinosa* (bee pollinated) was not included in the morphometric analyses because it has a radial symmetry.

bioRxiv preprint doi: https://doi.org/10.1101/041533; this version posted October 13, 2017. The copyright holder for this preprint (which was not certified by peer review) is the author/funder, who has granted bioRxiv a license to display the preprint in perpetuity. It is made available under aCC-BY-NC 4.0 International license.

Evolutionary models

Univariate models

For PC1 that captures variation in corolla opening, all models that received $AICc$ weights greater than zero suggest that the hummingbird specialists and the mixed-pollination species differed in their mean shape as they all included distinct θ for the two strategies (Table 2). The best models, OUM and BM1m ($AICc$ weight of 0.48 and 0.35, respectively), suggest that the two pollination strategies had similar evolutionary phenotypic variance as they constrain them to have identical parameters. This trend is also supported by parameter estimates of supported models that allowed the strategies to differ in drift rates (BMVm) or stationary variance (OUMV, OUMA, OUMVA) as these estimates were very similar for the two strategies (Table 2). The phylogenetic half-time of the OUM model, which corresponds to the time required for the expected phenotype to move half-way towards the optimal shape from its ancestral state (Hansen, 1997), was of 0.009. Given that the trees were scaled to unit height, this small value imply either very strong selective pressure or a lack of phylogenetic correlation. The results of the analyses that included species with inferred pollination strategies were almost identical in terms of model selection and phenotypic disparity (Table S6).

The PC2 of the morphospace that represents variation in the curve of the corolla was found to best fit a OUBMi model ($AICc$ weight = 0.72; Table 2), with the hummingbird pollinated species evolving under a OU model and the mixed-pollination species evolving under a BM model, each with their own drift rate implying that this model cannot be simply interpreted as reduced constraints for mixed-pollination species. Nevertheless, the model suggests that the pollination strategies have the same mean shape for PC2 and that the two pollination strategies have evolved under different types of constraints. The median phylogenetic half-time was of 0.02 for the hummingbird species, suggesting either very strong selective pressure or a lack of phylogenetic correlation. Parameter estimates for the other models, in particular the second best model OUMV ($AICc$ weight = 0.15), also supported similar mean shapes for the two pollination strategies and suggest that hummingbird pollinated species have greater phenotypic disparity as they have a greater stationary variance than mixed-pollination species (Table 2). The median phylogenetic half-time for the OUMV model was estimated

bioRxiv preprint doi: https://doi.org/10.1101/041533 This version posted October 13, 2017. The copyright holder for this preprint (which was not certified by peer review) is the author/funder, who has granted bioRxiv a license to display the preprint in perpetuity. It is made available under aCC-BY-NC 4.0 International license.

Table 2: Parameter values of the univariate evolutionary models fitted on the first three principal components of the morphospace when only the species with confirmed pollinators were included in the analyses. Mean values from the posterior distribution of species trees are given for the AICc weights, whereas median values are given for the parameter estimates. Numbers in brackets indicate the 25% and the 75% quantiles. The best model for each PC is in bold. The θ parameter indicate the global or regime means (ancestral states) for the BM-type and OUBM-type models, whereas it indicates the stationary optimum trait for the OU-type models. $station_{hum}$ and $station_{mix}$ are the stationary distributions of the hummingbird and mixed-pollination strategies.

PC1

Models	p	*AICc* weight	θ_{hum}	θ_{mix}	σ^2_{hum}	σ^2_{mix}	$station_{hum}$	$station_{mix}$
BM1	2	0 [0,0]	0.057 [0.05,0.066]	0.057 [0.05,0.066]	0.046 [0.037,0.074]	0.046 [0.037,0.074]	–	–
BMV	3	0 [0,0]	0.07 [0.011,0.113]	0.07 [0.011,0.113]	0.035 [0.02,0.093]	0.045 [0.026,0.086]	–	–
BM1m	3	0.35 [0.02,0.68]	0.15 [0.144,0.155]	-0.123 [-0.131,-0.112]	0.017 [0.013,0.023]	0.017 [0.013,0.023]	–	–
BMVm	4	0.1 [0.01,0.17]	0.146 [0.138,0.153]	-0.124 [-0.132,-0.112]	0.021 [0.014,0.031]	0.013 [0.012,0.016]	–	–
OU1	3	0 [0,0]	0.05 [0.039,0.057]	0.05 [0.039,0.057]	0.088 [0.061,0.197]	0.088 [0.061,0.197]	0.029 [0.029,0.031]	0.029 [0.029,0.031]
OUM	**4**	**0.48 [0.11,0.84]**	**0.16 [0.152,0.163]**	**-0.155 [-0.156,-0.152]**	**0.859 [0.265,3.004]**	**0.859 [0.265,3.004]**	**0.006 [0.006,0.006]**	**0.006 [0.006,0.006]**
OUMV	5	0.05 [0,0]	0.197 [0.18,0.222]	-0.134 [-0.226,-0.094]	8.248 [3.772,23.45]	7.442 [2.802,21.646]	2.684 [1.381,5.179]	2.696 [1.443,4.635]
OUMA	5	0.02 [0,0]	0.195 [0.178,0.23]	-0.14 [-0.246,-0.09]	8.935 [3.876,19.47]	8.935 [3.876,19.47]	2.573 [1.857,3.386]	2.667 [2.107,3.739]
OUMVA	6	0.01 [0,0]	0.195 [0.175,0.212]	-0.141 [-0.257,-0.106]	7.756 [3.12,23.395]	6.743 [2.518,18.899]	2.439 [1.388,4.782]	3.018 [1.516,4.646]
OUBMi	4	0 [0,0]	0.125 [0.106,0.142]	0.125 [0.106,0.142]	0.252 [0.065,4.186]	0.042 [0.023,0.064]	0.009 [0.007,0.013]	–
BMOUi	4	0 [0,0]	0.038 [-0.03,0.092]	0.038 [-0.03,0.092]	0.04 [0.021,0.095]	0.06 [0.032,0.104]	–	460558.818 [0.017,18[illegible]
OUBM	3	0 [0,0]	0.135 [0.12,0.151]	0.135 [0.12,0.151]	0.073 [0.056,0.13]	0.073 [0.056,0.13]	0.007 [0.006,0.009]	–
BMOU	3	0 [0,0]	0.043 [-0.045,0.059]	0.043 [-0.045,0.059]	0.053 [0.037,0.107]	0.053 [0.037,0.107]	–	18437.122 [0.009,55[illegible]77

PC2

Models	p	*AICc* weight	θ_{hum}	θ_{mix}	σ^2_{hum}	σ^2_{mix}	$station_{hum}$	$station_{mix}$
BM1	2	0 [0,0]	-0.035 [-0.037,-0.032]	-0.035 [-0.037,-0.032]	0.021 [0.013,0.038]	0.021 [0.013,0.038]	–	–
BMV	3	0.04 [0,0.04]	-0.035 [-0.041,-0.025]	-0.035 [-0.041,-0.025]	0.036 [0.021,0.065]	0 [0,0]	–	–
BM1m	3	0 [0,0]	-0.031 [-0.035,-0.028]	-0.041 [-0.048,-0.036]	0.021 [0.013,0.038]	0.021 [0.013,0.038]	–	–
BMVm	4	0.01 [0,0.01]	-0.028 [-0.036,-0.02]	-0.038 [-0.046,-0.026]	0.036 [0.02,0.064]	0 [0,0]	–	–
OU1	3	0.01 [0,0.02]	-0.036 [-0.036,-0.036]	-0.036 [-0.036,-0.036]	0.972 [0.18,1.104]	0.972 [0.18,1.104]	0.003 [0.003,0.003]	0.003 [0.003,0.003]
OUM	4	0 [0,0.01]	-0.042 [-0.044,-0.042]	-0.027 [-0.027,-0.026]	0.499 [0.107,1.041]	0.499 [0.107,1.041]	0.003 [0.003,0.003]	0.003 [0.003,0.003]
OUMV	5	0.15 [0.01,0.28]	-0.026 [-0.039,-0.014]	-0.017 [-0.04,-0.01]	10.239 [5.932,18.219]	0.018 [0,0.072]	1.663 [1.314,2.512]	0.003 [0,0.01]
OUMA	5	0 [0,0]	-0.024 [-0.04,-0.015]	-0.016 [-0.038,-0.005]	6.319 [3.531,11.251]	6.319 [3.531,11.251]	0.868 [0.671,1.145]	0.868 [0.671,1.145]
OUMVA	6	0.02 [0,0.03]	-0.025 [-0.038,-0.013]	-0.017 [-0.041,-0.011]	13.96 [6.714,26.595]	0.027 [0.001,1.106]	1.772 [1.316,3.017]	0.004 [0,0.167]
OUBMi	**4**	**0.72 [0.53,0.93]**	**-0.043 [-0.045,-0.041]**	**-0.043 [-0.045,-0.041]**	**0.305 [0.132,0.93]**	**0 [0,0]**	**0.004 [0.004,0.004]**	**–**
BMOUi	4	0.01 [0,0.01]	-0.035 [-0.041,-0.025]	-0.035 [-0.041,-0.025]	0.036 [0.021,0.065]	0.001 [0,0.001]	–	0 [0,0]
OUBM	3	0 [0,0]	-0.044 [-0.05,-0.035]	-0.044 [-0.05,-0.035]	0.03 [0.019,0.064]	0.03 [0.019,0.064]	0.003 [0.003,0.005]	–
BMOU	3	0.03 [0,0.02]	-0.029 [-0.038,-0.025]	-0.029 [-0.038,-0.025]	0.036 [0.021,0.064]	0.036 [0.021,0.064]	–	0 [0,0]

PC3

Models	p	*AICc* weight	θ_{hum}	θ_{mix}	σ^2_{hum}	σ^2_{mix}	$station_{hum}$	$station_{mix}$
BM1	2	0.06 [0.01,0.09]	0.017 [0.015,0.019]	0.017 [0.015,0.019]	0.005 [0.004,0.006]	0.005 [0.004,0.006]	–	–
BMV	3	0.02 [0,0.03]	0.017 [0.015,0.019]	0.017 [0.015,0.019]	0.005 [0.004,0.006]	0.005 [0.004,0.006]	–	–
BM1m	3	0.02 [0,0.03]	0.023 [0.022,0.026]	0.004 [0.001,0.007]	0.005 [0.004,0.005]	0.005 [0.004,0.005]	–	–
BMVm	4	0.01 [0,0.01]	0.024 [0.022,0.026]	0.004 [0.001,0.007]	0.005 [0.004,0.006]	0.005 [0.004,0.006]	–	–
OU1	3	0.18 [0.04,0.27]	0.013 [0.013,0.016]	0.013 [0.013,0.016]	0.036 [0.017,0.739]	0.036 [0.017,0.739]	0.002 [0.002,0.002]	0.002 [0.002,0.002]
OUM	4	0.05 [0.01,0.07]	0.015 [0.014,0.019]	0.012 [0.011,0.013]	0.03 [0.017,0.713]	0.03 [0.017,0.713]	0.002 [0.002,0.002]	0.002 [0.002,0.002]
OUMV	**5**	**0.36 [0.18,0.53]**	**0.027 [0.025,0.029]**	**0.014 [0.01,0.022]**	**13.351 [7.115,26.325]**	**3.692 [2.121,6.126]**	**1.033 [0.744,1.621]**	**0.291 [0.215,0.359]**
OUMA	5	0.12 [0.04,0.17]	0.026 [0.022,0.028]	0.017 [0.01,0.024]	4.885 [3.11,13.095]	4.885 [3.11,13.095]	0.505 [0.395,0.728]	0.505 [0.395,0.728]
OUMVA	6	0.04 [0.02,0.06]	0.027 [0.024,0.029]	0.014 [0.009,0.022]	6.412 [4.403,19.508]	2.492 [1.504,5.957]	0.734 [0.556,1.073]	0.264 [0.196,0.375]
OUBMi	4	0.01 [0,0.01]	0.015 [0.013,0.018]	0.015 [0.013,0.018]	0.012 [0.009,0.021]	0.005 [0.004,0.006]	0.002 [0.002,0.003]	–
BMOUi	4	0.04 [0.01,0.04]	0.015 [0.014,0.017]	0.015 [0.014,0.017]	0.005 [0.004,0.006]	0.041 [0.021,0.233]	–	0.001 [0.001,0.001]
OUBM	3	0.03 [0,0.04]	0.017 [0.014,0.02]	0.017 [0.014,0.02]	0.007 [0.006,0.009]	0.007 [0.006,0.009]	0.003 [0.002,0.004]	–
BMOU	3	0.07 [0.01,0.07]	0.015 [0.013,0.017]	0.015 [0.013,0.017]	0.006 [0.005,0.008]	0.006 [0.005,0.008]	–	0.001 [0.001,0.001]

bioRxiv preprint doi: https://doi.org/10.1101/041533; this version posted October 13, 2017. The copyright holder for this preprint (which was not certified by peer review) is the author/funder, who has granted bioRxiv a license to display the preprint in perpetuity. It is made available under aCC-BY-NC 4.0 International license.

to be 0.23, suggesting moderate constraints on corolla shape. The analyses including species with inferred pollination strategies best supported a OU1 model ($AICc$ weights = 0.69; Table S6) indicating a lack of evidence for different constraints or disparity for the two strategies. But in models where the evolutionary rate of stationary variance was allowed to vary between strategies, the hummingbird pollinated species showed higher variance than the mixed-pollinated species (Table S6).

The PC3 that represents variation in the reflexion of the petal lobes was found to best fit a OUMV model ($AICc$ weight = 0.36), although models OU1 and OUMA also received considerable weights ($AICc$ weights of 0.18 and 0.12, respectively; Table 2). All three models suggest that this shape component tend to stay closer to the evolutionary mean than would be expected under a BM model. The OU1 suggests that the pollination strategies have the same mean shape, whereas the OUM and OUMV models suggest different mean shapes, although parameter estimates for these later models showed that the mean shapes for both strategies are not very far from each other (Table 2). The models OUMV and OUMA suggest different shape disparity with the hummingbird specialists having a higher stationary variance than mixed-pollination species. The models OUMV, OU1 and OUMA all suggested strong constraints with estimated phylogenetic half-times of 0.11, 0.08, and 0.14, respectively. In analyses with species with inferred pollination strategies, the OU1 model received the highest weight (0.30), although several models received weights greater than 0.05 (Table S6). As for the analyses with only species with confirmed pollination strategies, the hummingbird pollinated species showed higher stationary variance in models in which this parameter was allowed to vary between strategies (Table S6).

In some instances, the models OU1 and OUM did not always converge to the maximum likelihood solution when fitted with `OUwie`, especially for PC1. This is why we always fitted these models with `mvMORPH`, which is also faster. Similarly, the models OUMV, OUMA, and OUMVA showed relatively poor convergence and should be interpreted with caution.

Multivariate models

The multivariate analyses supported OUM as the best fitting model ($AICc$ weight = 0.60; Table 3). This model suggests that the shape components have different evolutionary means

bioRxiv preprint doi: https://doi.org/10.1101/041533; this version posted October 13, 2017. The copyright holder for this preprint (which was not certified by peer review) is the author/funder, who has granted bioRxiv a license to display the preprint in perpetuity. It is made available under aCC-BY-NC 4.0 International license.

for the two pollination strategies and that there is an evolutionary force that maintains the corolla shape closer to this evolutionary mean than would be expected under a BM model. The shape means estimated under the multivariate OUM model for each PC were very similar to that of the univariate estimates, as were the estimates of the stationary variance and phylogenetic halftimes (compare Tables 2 and 4). The stationary variance estimates were also similar to the observed variance among species for hummingbird pollinated species (PC1: 0.0068, PC2: 0.0049, PC3: 0.0041) and mixed-pollinated species (PC1: 0.0075, PC2: 0.0014, PC3: 0.0016), suggesting that the model is very close to be stationary.

Because the current implementation do not allow the estimation of regime-specific evolutionary correlations between traits under the multivariate OUM model, we looked at the evolutionary correlations between drift rates (σ^2) under the BMVm model, which was the third best supported model ($AICc$ weight = 0.13; Table 3), to estimate the morphological integration for the two pollination strategies. The evolutionary correlations between shape components were always greater for the mixed-pollination strategy in terms of absolute correlation, although there is some uncertainty in these estimates as evident from the 50% posterior intervals (Fig. 4). Furthermore, the better support for the OUM and BM1m models also suggests that differences between pollination strategies are probably marginal or that we lack statistical power to detect significant differences. Because these correlations were obtained on a BMVm model whereas a OUM model was the one that received the highest support, there is a risk that the younger mixed-pollination clades may appear to have evolved faster under the BMVm model (Price et al., 2013), which could in turn affect the observed correlations. However, this does not seem to be the case as the correlations estimated on data simulated with the OUM model were similar between pollination strategies (Fig. 4), rejecting the possibility that the greater absolute correlations observed for the mixed-pollination strategy were due to model mis-specification. The multivariate results obtained when species with inferred pollinators were included were similar, with even more support for the OUM model ($AICc$ weight = 1; Table S8, S9). However, the correlation between traits suggest phenotypic integration of more similar amplitude for the two pollination strategies with inferred pollinators (Fig. S2); these differences could be due to the small sample sizes as such correlations are difficult to estimate accurately.

bioRxiv preprint doi: https://doi.org/10.1101/041533; this version posted October 13, 2017. The copyright holder for this preprint (which was not certified by peer review) is the author/funder, who has granted bioRxiv a license to display the preprint in perpetuity. It is made available under aCC-BY-NC 4.0 International license.

Table 3: Model performance with the multivariate evolutionary models fitted on the first three principal components of the morphospace when only confirmed species are included in the analyses. The mean values obtained from the posterior distribution of species trees are given; numbers in brackets indicate the 25% and the 75% quantiles. The best model is in bold.

Models	*logLik*	Parameters	*AICc* weight
BM1	67.98 [63.43,76.25]	9	0.00 [0.00,0.00]
BMV	80.44 [76.94,86.18]	15	0.00 [0.00,0.00]
BM1m	78.52 [72.7,86.95]	12	0.24 [0.00,0.45]
BMVm	90.47 [85.96,96.59]	18	0.13 [0.00,0.12]
OU1	82.30 [74.47,87.04]	15	0.02 [0.00,0.00]
OUM	**96.24 [93.47,98.18]**	**18**	**0.60 [0.03,1.00]**
OUBM	77.17 [74.14,82.47]	15	0.00 [0.00,0.00]
BMOU	80.47 [76.97,85.85]	15	0.01 [0.00,0.00]
OUBMi	95.24 [93.99,97.05]	21	0.01 [0.00,0.00]
BMOUi	83.71 [80.01,89.11]	21	0.00 [0.00,0.00]

Table 4: Model parameters for the multivariate OUM model, which was the model that received the highest *AICc* weight (Table 3). The mean values obtained from the posterior distribution of species trees are given; numbers in brackets indicate the 25% and the 75% quantiles. The complete stationary variance matrix is given in Table S7.

parameters	PC1	PC2	PC3
θ_{hum}	0.161 [0.152,0.166]	-0.043 [-0.046,-0.042]	0.013 [0.009,0.015]
θ_{mix}	-0.156 [-0.159,-0.154]	-0.026 [-0.027,-0.023]	0.013 [0.012,0.02]
σ^2	1.198 [0.135,0.135]	1.328 [0.184,0.184]	0.757 [0.005,0.005]
Phylogenetic halftime	0.002 [0.001,0.003]	0.01 [0.003,0.031]	0.101 [0.01,0.194]
Stationary variance	0.006 [0.005,0.006]	0.003 [0.003,0.003]	0.002 [0.002,0.002]

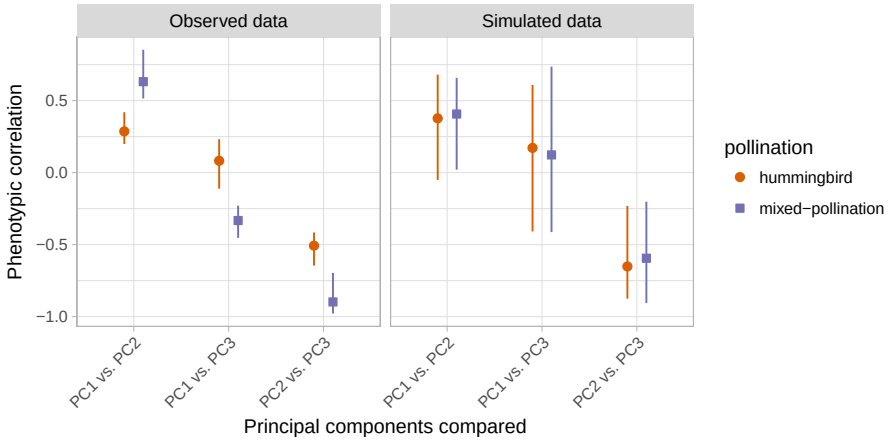

Figure 4: Graphical representation of the evolutionary correlations (i.e., standardized evolutionary rates matrices) obtained with the BMVm multivariate model with only species with confirmed pollination strategies, for the observed data (left panel) and for data simulated under the best fitting model (OUM; right panel). Symbols represent the median correlation and the lines the 25% and 75% quantiles for both hummingbirds and mixed-pollination strategies. No artifactual differences are detected between the two groups when fitting models on traits simulated with the OUM model and thus with a common evolutionary covariance (right panel, see text).

bioRxiv preprint doi: https://doi.org/10.1101/041533; this version posted October 13, 2017. The copyright holder for this preprint (which was not certified by peer review) is the author/funder, who has granted bioRxiv a license to display the preprint in perpetuity. It is made available under aCC-BY-NC 4.0 International license.

Discussion

Although many aspects of the flower are required for assuring successful reproduction, the corolla shape is critical for the adaptation of plants to pollinators. In many species, the corolla guides the pollinator to allow precise pollen deposition on its body (Muchhala, 2007). But pollinators can also show an inherent preference for some floral shapes (Gómez et al., 2008) and can associate shape and reward when these are correlated (Meléndez-Ackerman et al., 1997). Floral shape has in fact repeatedly been shown to be under selection in pollination-driven selection studies (Galen, 1989; Campbell et al., 1991; O'Connell and Johnston, 1998; Maad, 2000) and can be sufficient to impose adaptive trade-off between pollinators (Muchhala, 2007). Even the corolla shape of super generalist species has been shown to adapt to particular guilds of pollinators (Gómez and Perfectti, 2010; Gómez et al., 2015).

In the Antillean genera *Gesneria* and *Rhytidophyllum*, pollination syndromes are well characterized and have good predictive value (Martén-Rodríguez et al., 2009), but previous studies were based on attractive and mechanical floral characters. Our results based on geometric morphometrics showed that it is possible to distinguish corollas of hummingbird pollinated species from moth pollinated species, and, although to a lesser degree, the corolla shapes of species with bat or mixed-pollination strategies. These conclusions were reinforced by the strong support in favour of distinct shapes for hummingbird specialists and mixed-pollination species in evolutionary models, both based on parameter estimates and on support for models supporting different evolutionary shape means (BMm models) or distinct shape optima (OUM models). These results, in addition to the fact that each pollination strategy evolved repeatedly in the Gesneriinae, further support the concept of pollination syndromes in this group and underlines the importance of corolla shape in floral adaptation to pollinators.

Long-term evolutionary constraints on corolla shape

If several studies estimated selection pressures on flowers within populations, few have addressed the question at macroevolutionary scales (but see Gómez et al., 2015). We hypothesized, based on theoretical expectations and empirical results, that the corolla shape of flowers should have evolved under evolutionary contraints to maintain effective pollination,

bioRxiv preprint doi: https://doi.org/10.1101/041533; this version posted October 13, 2017. The copyright holder for this preprint (which was not certified by peer review) is the author/funder, who has granted bioRxiv a license to display the preprint in perpetuity. It is made available under aCC-BY-NC 4.0 International license.

thereby reducing the phenotypic variance among species, and that this variance should be smaller for more specialist species because they are potentially under a more constant and precise selective pressure.

All analyses performed, both univariate and multivariate and using only species with confirmed pollinator information or also including species with inferred strategies, selected OU models that possess a α parameter that maintains the corolla shape closer to an evolutionary optimum. This supports the hypothesis that the corolla shape in the group has been affected by long-term evolutionary constraints, which could be interpreted as a consequence of the selective pressure imposed by pollinators. However, the analyses found very small phylogenetic halftimes, which are suggestive of very strong selection pressures and/or lack of phylogenetic correlation in the data (note that a strong impact of selection will necessarily reduce the phylogenetic correlation in the data). Considering a potential origin of the group ca. 10 mya (Roalson et al., 2008; Roalson and Roberts, 2016) and taking the smallest phylogenetic halftime obtained (0.002, for the PC1 in the multivariate analysis; Table 4), this means that a corolla shape can move half-way to its optimal shape in $0.002 \times 10 = 0.02$ million years, or 20,000 years. This is rapid, but not impossible considering that transitions between pollination strategies are generally driven by few genes of major effects (Galliot et al., 2006; Yuan et al., 2013). These small phylogenetic halftimes can also imply a lack of phylogenetic influence, but given that the corolla shape is clearly under genetic control in the group (Alexandre et al., 2015), this seems less plausible.

Contrarily to our initial hypothesis, we did not find evidence that pollination specialist species show reduced phenotypic disparity compared to mixed-pollination species. The non-phylogenetic approaches suggested similar amount of variation among species for both pollination strategies, and this pattern was confirmed by the evolutionary models. Indeed, almost all analyses selected a model in which both strategies evolved under shared constraints, but for different means for each selective regime. Moreover, although the differences were marginal, the parameter estimates of the evolutionary models that allows the two strategies to have different phenotypic disparities almost constantly indicated that it was the hummingbird specialists that showed a higher disparity compared to the more generalist mixed-pollination species.

bioRxiv preprint doi: https://doi.org/10.1101/041533; this version posted October 13, 2017. The copyright holder for this preprint (which was not certified by peer review) is the author/funder, who has granted bioRxiv a license to display the preprint in perpetuity. It is made available under aCC-BY-NC 4.0 International license.

Morphological integration and evolutionary correlations between shape components allows us to take another view at evolutionary contraints on corolla shape. Indeed, important integration between the shape components suggests tight coordination for proper functioning and strong evolutionary correlations suggest that components have evolved in an highly coordinated fashion. The results showed both higher morphological integration and evolutionary correlations for the mixed-pollination species, which goes against the generally accepted idea that more generalist species are less constrained. Overall, we come to the conclusion that greater generalization in pollination strategies did not imply a relaxation of evolutionary constraints over macroevolutionary scales in Antillean Gesneriinae.

How can we explain that we did not observe more phenotypic disparity for the mixed-pollination strategy? Although any answer to this question is necessarily tentative at this point, a potential line of enquiry could be associated with the process by which the species become generalized. One such process, which we call the compromised phenotype and that motivated our initial hypotheses, is that generalists evolve by becoming intermediate in morphology relative to specialist species (Fig. 5). This could occur in the presence of weak or non-symmetric trade-off effects if both pollinators are present (Aigner, 2001, 2006; Sahli and Conner, 2011). Under such a scenario, the floral variation of generalists could span the whole region between the shapes of the two specialists either because of drift or because of variation in the the relative contribution of the different pollinators for each species. This could result in a relatively broad variation among species compared to that of specialists; but this is not what we observe here.

An alternative, called the specialized phenotype, is that the generalists occupy a distinct region in the phenotypic landscape (Fig. 5). Under this scenario, the morphological variance in floral shape need not be greater than that of specialists as generalists could have a floral morphology optimized to both types of pollinators. This model may fit well to the present group as it has been suggested that the presence of a constriction at the base of the corolla for species with a mixed-pollination strategy could represent an adaptation to allow a good pollination service by both hummingbirds and bats by forcing them to approach the flower in a specific way (Martén-Rodríguez et al., 2009). The fact that the corolla shape typical of this pollination strategy has evolved recurrently in the group (Fig. 2) certainly adds weight to

bioRxiv preprint doi: https://doi.org/10.1101/041533; this version posted October 13, 2017. The copyright holder for this preprint (which was not certified by peer review) is the author/funder, who has granted bioRxiv a license to display the preprint in perpetuity. It is made available under aCC-BY-NC 4.0 International license.

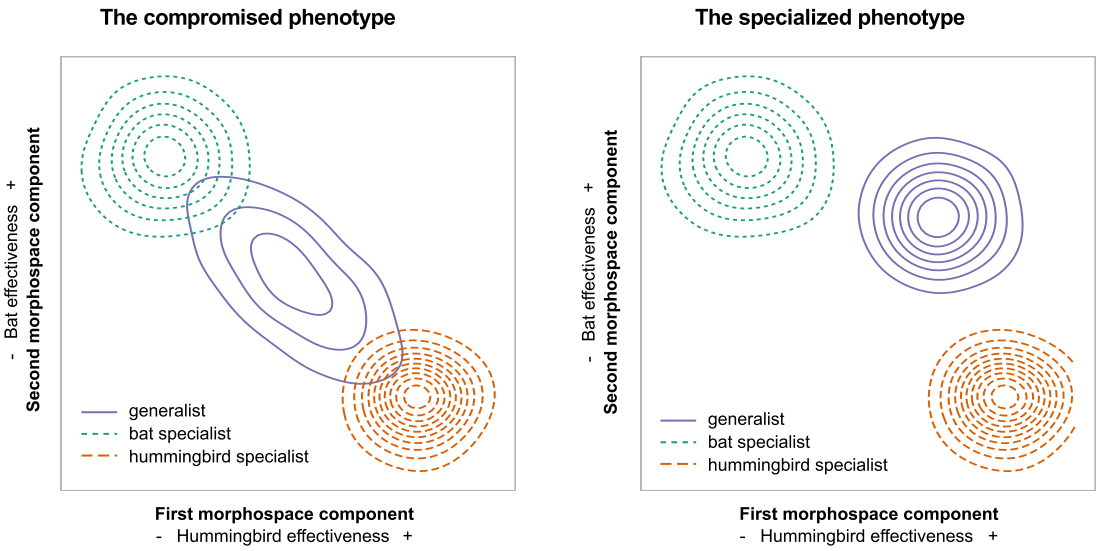

Figure 5: Conceptual phenotypic landscapes illustrating the distribution in mean phenotype of ecological specialist and generalist species associated with two scenarios of evolution of generalization. The x- and y-axis are associated with increases in hummingbird and bat pollination effectiveness, respectively. This is clearly an oversimplified example as real morphospaces are multi-dimensional and the relationship between pollination effectiveness and morphology more complex. In the **compromised phenotype** scenario, the generalists are intermediate in morphology between the two specialists and have the potential to occupy the full extent of variation between the two extremes. In such a scenario, the generalists can have greater variance in morphology and pollination effectiveness than specialists. In the **specialized phenotype** scenario, the generalists occupy a completely distinct region of the morphological landscape; they do not (necessarily) show increased morphological variance compared to specialists and shows good pollination effectiveness by both types of pollinators.

this hypothesis. These mixed-pollination species might thus have a phenotypically specialized corolla, in the sense that it is well adapted to both bat and hummingbird pollination, even though they are ecological generalists by being pollinated by different functional pollinators. Indeed, concepts of phenotypic specialization and ecological specialization need not be correlated (Ollerton et al., 2007; Fleming and Muchhala, 2008; Armbruster, 2014). This strategy might be particularly successful in fine-grained pollination environment (Aigner, 2006), such as where pollinators are scarce or vary through time (Waser et al., 1996). Such hypothesis of adaptive generalization (see Gómez and Zamora, 2006) certainly deserves more attention in the future, and will require information on pollination frequency and efficiency to properly associate flower shape to the relative efficiency of pollinators.

The detection of selection contraints for both pollination strategies is noteworthy given that several factors probably contribute in reducing this signal over macroevolutionary timescales.

bioRxiv preprint doi: https://doi.org/10.1101/041533; this version posted October 13, 2017. The copyright holder for this preprint (which was not certified by peer review) is the author/funder, who has granted bioRxiv a license to display the preprint in perpetuity. It is made available under aCC-BY-NC 4.0 International license.

For instance, temporal variation in pollination guilds over macroevolutionary times could weaken the signal of selection, mirroring observations at the population level (e.g., Campbell, 1989; Campbell et al., 1991). The pollination guilds were assumed to be functionally constant over time in our analyses. But given that the exact species pollinating the flowers vary among plant species (Martén-Rodríguez et al., 2009, 2015), the whole story might be more complex. For instance, unrecognized sub-syndromes could be responsible for the larger variation observed for the hummingbird strategy and additional pollinator information will be needed to investigate this further. Variation in selective pressure among species could also occur if agents other than pollinators affect corolla shape. For instance, the apical constriction of the corolla of hummingbird pollinated *Drymonia* (Gesneriaceae) has recently been suggested to be an adaptation to exclude bees (Clark et al., 2015). Moreover, herbivores, including nectar robbers, may affect the selective forces imposed on flowers by pollinators (e.g., Galen and Cuba, 2001; Gómez, 2003). While non-pollinating floral visitors–including bees–are generally not abundant in the group (Martén-Rodríguez et al., 2009, 2015) and herbivory is not common (pers. obs.), it is difficult to completely discard this possibility.

This study is one of the first to show evidence of constrained evolution on flower shapes imposed by pollinator guilds over macroevolutionary time scales and demonstrates the usefulness of a phylogenetic approach to understand pollinator mediated selection. Although additional investigations are needed to confirm these patterns, this study certainly adds weight to the evidence accumulated by many others over the years that the specialist - generalist continuum in pollination biology is complex (Waser et al., 1996; Waser and Ollerton, 2006) and that we cannot assume a priori that pollination specialists show reduced phenotypic disparity compared to pollination generalists.

Supplementary figures and tables

The supplementary figures and table are available with the supplementary material that is associated with this manuscript. The interactive supplementary figures can be visualized here: `www.plantevolution.org/data/Joly_2017_SuppFigs.html`.

bioRxiv preprint doi: https://doi.org/10.1101/041533; this version posted October 13, 2017. The copyright holder for this preprint (which was not certified by peer review) is the author/funder, who has granted bioRxiv a license to display the preprint in perpetuity. It is made available under aCC-BY-NC 4.0 International license.

Authors contributions

SJ conceived the study. FL, HA, ELB and JLC collected the data, SJ, FL and JC analyzed the data, SJ wrote the draft and all authors contributed and critically edited the final manuscript.

Acknowledgements

We thank William Cinea and Phito Merizier that significantly contributed to making this work possible, Julie Faure for constructive discussions, and Cécile Ané for comments and suggestions on a previous manuscript. We also acknowledge the help of Calcul Québec and the Genome Québec Innovation Centre.

Funding

Funding to JLC was provided by a Research and Exploration grant from the National Geographic Society (9522-14). This study was financially supported by the Quebec Centre for Biodiversity Science (QCBS) and by a Discovery Grant to SJ from the Natural Sciences and Engineering Research Council of Canada (402363-2011).

References

Adams, D. C. and E. Otárola-Castillo, 2013. geomorph: an R package for the collection and analysis of geometric morphometric shape data. Methods Ecol Evol 4:393–399.

Aigner, P. A., 2001. Optimality modeling and fitness trade-offs: when should plants become pollinator specialists? Oikos 95:177–184.

———, 2006. The evolution of specialized floral phenotypes in a fine-grained pollination environment. Pp. 23–46, *in* N. M. Waser and J. Ollerton, eds. Plant-pollinator interactions: from specialization to generalization. University of Chicago Press, Chicago.

Alexandre, H., J. Vrignaud, B. Mangin, and S. Joly, 2015. Genetic architecture of pollination syndrome transition between hummingbird-specialist and generalist species in the genus *Rhytidophyllum* (Gesneriaceae). PeerJ 3:e1028.

Armbruster, W. S., 2014. Floral specialization and angiosperm diversity: phenotypic divergence, fitness trade-offs and realized pollination accuracy. AoB PLANTS 6:plu003.

bioRxiv preprint doi: https://doi.org/10.1101/041533; this version posted October 13, 2017. The copyright holder for this preprint (which was not certified by peer review) is the author/funder, who has granted bioRxiv a license to display the preprint in perpetuity. It is made available under aCC-BY-NC 4.0 International license.

Ashman, T.-L. and C. J. Majetic, 2006. Genetic constraints on floral evolution: a review and evaluation of patterns. Heredity 96:343–352.

Baker, H. G., 1961. The adaptation of flowering plants to nocturnal and crepuscular pollinators. The Quarterly Review of Biology 36:64–73.

Beaulieu, J. M., D.-C. Jhwueng, C. Boettiger, and B. C. O'Meara, 2012. Modeling stabilizing selection: expanding the Ornstein-Uhlenbeck model of adaptive evolution. Evolution 66:2369–2383.

Boberg, E., R. Alexandersson, M. Jonsson, J. Maad, J. Ågren, and L. A. Nilsson, 2014. Pollinator shifts and the evolution of spur length in the moth-pollinated orchid *Platanthera bifolia*. Ann Bot 113:267–275.

Bookstein, F. L., 1997. Landmark methods for forms without landmarks: morphometrics of group differences in outline shape. Medical Image Analysis 1:225–243.

Boucher, F. C. and V. Démery, 2016. Inferring bounded evolution in phenotypic characters from phylogenetic comparative data. Syst Biol 65:651–661.

Breitkopf, H., R. E. Onstein, D. Cafasso, P. M. Schlüter, and S. Cozzolino, 2015. Multiple shifts to different pollinators fuelled rapid diversification in sexually deceptive *Ophrys* orchids. New Phytol 207:377–389.

Burnham, K. P. and D. R. Anderson, 2002. Model selection and multimodel inference: a practical information-theoretic approach. 2nd edition ed. Springer, New York.

Butler, M. and A. King, 2004. Phylogenetic comparative analysis: a modeling approach for adaptive evolution. The American Naturalist 164:683–695.

Campbell, D. R., 1989. Measurements of selection in a hermaphroditic plant: variation in male and female pollination success. Evolution 43:318–334.

Campbell, D. R., N. M. Waser, M. V. Price, E. A. Lynch, and R. J. Mitchell, 1991. Components of phenotypic selection: pollen export and flower corrolla width in *Ipomopsis aggregata*. Evolution 45:1458–1467.

Castresana, J., 2000. Selection of conserved blocks from multiple alignments for their use in phylogenetic analysis. Molecular Biology and Evolution 17:540–552.

Clark, J. L., L. Clavijo, and N. Muchhala, 2015. Convergence of anti-bee pollination mechanisms in the Neotropical plant genus Drymonia (Gesneriaceae). Evol Ecol 29:355–377.

Clavel, J., G. Escarguel, and G. Merceron, 2015. mvMORPH: an R package for fitting multivariate evolutionary models to morphometric data. Methods Ecol Evol 6:1311–1319.

bioRxiv preprint doi: https://doi.org/10.1101/041533; this version posted October 13, 2017. The copyright holder for this preprint (which was not certified by peer review) is the author/funder, who has granted bioRxiv a license to display the preprint in perpetuity. It is made available under aCC-BY-NC 4.0 International license.

Conner, J. K., A. M. Rice, C. Stewart, and M. T. Morgan, 2003. Patterns and mechanisms of selection on a family-diagnostic trait: evidence from experimental manipulation and lifetime fitness selection gradients. Evolution 57:480–486.

Cooper, N., G. H. Thomas, C. Venditti, A. Meade, and R. P. Freckleton, 2016. A cautionary note on the use of Ornstein Uhlenbeck models in macroevolutionary studies. Biol. J. Linn. Soc. 118:64–77.

Crepet, W. L., 1984. Advanced (constant) insect pollination mechanisms: pattern of evolution and implications vis-a-vis angiosperm diversity. Annals of the Missouri Botanical Garden 71:607–630.

Cresswell, J. E., 1998. Stabilizing selection and the structural variability of flowers within species. Ann Bot 81:463–473.

Darriba, D., G. L. Taboada, R. Doallo, and D. Posada, 2012. jModelTest 2: more models, new heuristics and parallel computing. Nature Methods 9:772–772.

Drummond, A. J., M. A. Suchard, D. Xie, and A. Rambaut, 2012. Bayesian phylogenetics with BEAUti and the BEAST 1.7. Mol Biol Evol .

Faegri, K. and L. van der Pijl, 1979. The Principles of Pollination Ecology. Pergamon Press, Oxford, UK.

Felsenstein, J., 1985. Phylogenies and the comparative method. The American Naturalist 125:1–15.

———, 1988. Phylogenies and quantitative characters. Ann. Rev. Ecol. Syst. 19:445–471.

Fenster, C. B., W. S. Armbruster, P. Wilson, M. R. Dudash, and J. D. Thomson, 2004. Pollination syndromes and floral specialization. Annu. Rev. Ecol. Evol. Syst. 35:375–403.

Fleming, T. H. and N. Muchhala, 2008. Nectar-feeding bird and bat niches in two worlds: pantropical comparisons of vertebrate pollination systems. Journal of Biogeography 35:764–780.

Flemming, T. H., N. Muchhala, and J. F. Ornelas, 2005. New world nectar-feeding vertebrates: community patterns and processes. Pp. 163–186, *in* V. Sánchez-Cordero and R. Medellí, eds. Contribuciones mastozoológicas en homenaje a Bernardo Villa. UNAM, México.

Forest, F., P. Goldblatt, J. C. Manning, D. Baker, J. F. Colville, D. S. Devey, S. Jose, M. Kaye, and S. Buerki, 2014. Pollinator shifts as triggers of speciation in painted petal irises (Lapeirousia: Iridaceae). Ann Bot 113:357–371.

Galen, C., 1989. Measuring pollinator-mediated selection on morphometric floral traits: bumblebees and the alpine sky pilot, *Polemonium viscosum*. Evolution 43:882–890.

bioRxiv preprint doi: https://doi.org/10.1101/041533; this version posted October 13, 2017. The copyright holder for this preprint (which was not certified by peer review) is the author/funder, who has granted bioRxiv a license to display the preprint in perpetuity. It is made available under aCC-BY-NC 4.0 International license.

Galen, C. and J. Cuba, 2001. Down the tube: pollinators, predators, and the evolution of flower shape in the alpine skypilot, *Polemonium viscosum*. Evolution 55:1963–1971.

Galliot, C., J. Stuurman, and C. Kuhlemeier, 2006. The genetic dissection of floral pollination syndromes. Curr. Opin. Plant Biol. 9:78–82.

Gascuel, O. and M. Steel, 2014. Predicting the ancestral character changes in a tree is typically easier than predicting the root state. Syst Biol 63:421–435.

Gómez, J., 2003. Herbivory reduces the strength of pollinator-mediated selection in the Mediterranean herb *Erysimum mediohispanicum*: consequences for plant specialization. The American Naturalist 162:242–256.

Gómez, J. M., J. Bosch, F. Perfectti, J. D. Fernández, M. Abdelaziz, and J. P. M. Camacho, 2008. Spatial variation in selection on corolla shape in a generalist plant is promoted by the preference patterns of its local pollinators. Proc. R. Soc. B 275:2241–2249.

Gómez, J. M. and F. Perfectti, 2010. Evolution of complex traits: the case of *Erysimum* corolla shape. International Journal of Plant Sciences 171:987–998.

Gómez, J. M., F. Perfectti, and J. Lorite, 2015. The role of pollinators in floral diversification in a clade of generalist flowers. Evolution 69:863–878.

Gómez, J. M. and R. Zamora, 2006. Ecological factors that promote the evolution of generalization in pollination systems. Pp. 145–165, *in* Plant-pollinator interactions, from specialization to generalization. University of Chicago Press.

Haller, B. C. and A. P. Hendry, 2014. Solving the paradox of stasis: squashed stabilizing selection and the limits of detection. Evolution 68:483–500.

Hansen, T. F., 1997. Stabilizing selection and the comparative analysis of adaptation. Evolution 51:1341–1351.

Hansen, T. F. and E. P. Martins, 1996. Translating between microevolutionary process and macroevolutionary patterns: the correlation structure of interspecific data. Evolution 50:1404–1417.

Harmon, L. J., J. T. Weir, C. D. Brock, R. E. Glor, and W. Challenger, 2008. GEIGER: investigating evolutionary radiations. Bioinformatics 24:129–131.

Herrera, C. M., 1988. Variation in mutualisms: the spatiotemporal mosaic of a pollinator assemblage. Biological Journal of the Linnean Society 35:95–125.

Huelsenbeck, J. P., R. Nielsen, and J. P. Bollback, 2003. Stochastic mapping of morphological characters. Syst Biol 52:131–158.

bioRxiv preprint doi: https://doi.org/10.1101/041533; this version posted October 13, 2017. The copyright holder for this preprint (which was not certified by peer review) is the author/funder, who has granted bioRxiv a license to display the preprint in perpetuity. It is made available under aCC-BY-NC 4.0 International license.

Johnson, S. D., 2010. The pollination niche and its role in the diversification and maintenance of the southern African flora. Philos Trans R Soc Lond B Biol Sci 365:499–516.

Johnson, S. D. and K. E. Steiner, 2000. Generalization versus specialization in plant pollination systems. Trends in Ecology & Evolution 15:140–143.

Katoh, K. and D. M. Standley, 2013. MAFFT multiple sequence alignment software version 7: improvements in performance and usability. Mol Biol Evol 30:772–780.

Klingenberg, C. P., 2013. Cranial integration and modularity: insights into evolution and development from morphometric data. Hystrix 24:43–58.

Lande, R., 1976. Natural selection and random genetic drift in phenotypic evolution. Evolution 30:314–334.

———, 1979. Quantitative genetic analysis of multivariate evolution, applied to brain: body size allometry. Evolution 33:402–416.

Maad, J., 2000. Phenotypic selection in hawkmoth-pollinated *Platanthera bifolia*: targets and fitness surfaces. Evolution 54:112–123.

Martén-Rodríguez, S., A. Almarales-Castro, and C. B. Fenster, 2009. Evaluation of pollination syndromes in Antillean Gesneriaceae: evidence for bat, hummingbird and generalized flowers. Journal of Ecology 97:348–359.

Martén-Rodríguez, S. and C. B. Fenster, 2008. Pollination ecology and breeding systems of five *Gesneria* species from Puerto Rico. Ann Bot 102:23–30.

Martén-Rodríguez, S., C. B. Fenster, I. Agnarsson, L. E. Skog, and E. A. Zimmer, 2010. Evolutionary breakdown of pollination specialization in a caribbean plant radiation. New Phytologist 188:403–417.

Martén-Rodríguez, S., W. J. Kress, E. J. Temeles, and E. Meléndez-Ackerman, 2011. Plant-pollinator interactions and floral convergence in two species of *Heliconia* from the Caribbean Islands. Oecologia 167:1075–1083.

Martén-Rodríguez, S., M. Quesada, A.-A. Castro, M. Lopezaraiza-Mikel, and C. B. Fenster, 2015. A comparison of reproductive strategies between island and mainland Caribbean Gesneriaceae. J Ecol 103:1190–1204.

Medan, D., A. M. Basilio, M. Devoto, N. J. Bartoloni, J. P. Torretta, and T. Petanidou, 2006. Measuring generalization and connectance in temperate, year-long active systems. Pp. 245–259, *in* Plant-pollinator interactions: from specialization to generalization. The University of Chicago Press, Chicago.

Meléndez-Ackerman, E., D. R. Campbell, and N. M. Waser, 1997. Hummingbird behavior and mechanisms of selection on flower color in *Ipomopsis*. Ecology 78:2532–2541.

bioRxiv preprint doi: https://doi.org/10.1101/041533; this version posted October 13, 2017. The copyright holder for this preprint (which was not certified by peer review) is the author/funder, who has granted bioRxiv a license to display the preprint in perpetuity. It is made available under aCC-BY-NC 4.0 International license.

Muchhala, N., 2006. The pollination biology of *Burmeistera* (Campanulaceae): specialization and syndromes. Am. J. Bot. 93:1081–1089.

———, 2007. Adaptive trade-off in floral morphology mediates specialization for flowers pollinated by bats and hummingbirds. Am. Nat. 169:494–504.

Newman, E., B. Anderson, and S. D. Johnson, 2012. Flower colour adaptation in a mimetic orchid. Proc. R. Soc. B 279:2309–2313.

Newman, E., J. Manning, and B. Anderson, 2014. Matching floral and pollinator traits through guild convergence and pollinator ecotype formation. Ann Bot 113:373–384.

van der Niet, T. and S. D. Johnson, 2012. Phylogenetic evidence for pollinator-driven diversification of angiosperms. Trends in Ecology & Evolution 27:353–361.

Niet, T. V. d., M. D. Pirie, A. Shuttleworth, S. D. Johnson, and J. J. Midgley, 2014. Do pollinator distributions underlie the evolution of pollination ecotypes in the Cape shrub *Erica plukenetii*? Ann Bot 113:301–316.

O'Connell, L. M. and M. O. Johnston, 1998. Male and female pollination success in a deceptive orchid, a selection study. Ecology 79:1246–1260.

Oksanen, J., F. G. Blanchet, M. Friendly, R. Kindt, P. Legendre, D. McGlinn, P. R. Minchin, R. B. O'Hara, G. L. Simpson, P. Solymos, M. H. H. Stevens, E. Szoecs, and H. Wagner, 2017. vegan: Community Ecology Package. URL `http://CRAN.R-project.org/package=vegan`. R package version 2.4-2.

Ollerton, J., A. Killick, E. Lamborn, S. Watts, and M. Whiston, 2007. Multiple meanings and modes: on the many ways to be a generalist flower. Taxon 56:717–728.

O'Meara, B. C., C. Ané, M. J. Sanderson, and P. C. Wainwright, 2006. Testing for different rates of continuous trait evolution using likelihood. Evol 60:922.

Pavlicev, M., J. M. Cheverud, and G. P. Wagner, 2009. Measuring morphological integration using eigenvalue variance. Evol Biol 36:157–170.

Perret, M., A. Chautems, R. Spichiger, T. G. Barraclough, and V. Savolainen, 2007. The geographical pattern of speciation and floral diversification in the Neotropics: the tribe Sinningieae (Gesneriaceae) as a case study. Evolution 61:1641–1660.

Price, S. A., J. J. Tavera, T. J. Near, and P. C. Wainwright, 2013. Elevated rates of morphological and functional diversification in reef-dwelling Haemulid fishes. Evolution 67:417–428.

R core team, 2014. R: a language and environment for statistical computing. URL `http://www.R-project.org`.

bioRxiv preprint doi: https://doi.org/10.1101/041533; this version posted October 13, 2017. The copyright holder for this preprint (which was not certified by peer review) is the author/funder, who has granted bioRxiv a license to display the preprint in perpetuity. It is made available under aCC-BY-NC 4.0 International license.

Revell, L. J., 2012. phytools: an R package for phylogenetic comparative biology (and other things). Methods in Ecology and Evolution 3:217–223.

———, 2013. A comment on the use of stochastic character maps to estimate evolutionary rate variation in a continuously valued trait. Syst. Biol. 62:339–345.

Revell, L. J. and D. C. Collar, 2009. Phylogenetic analysis of the evolutionary correlation using likelihood. Evolution 63:1090–1100.

Roalson, E. H. and W. R. Roberts, 2016. Distinct processes drive diversification in different clades of Gesneriaceae. Syst Biol 65:662–684.

Roalson, E. H., L. E. Skog, and E. A. Zimmer, 2008. Untangling Gloxinieae (Gesneriaceae). II. Reconstructing biogeographic patterns and estimating divergence times among New World continental and island lineages. Systematic Botany 33:159–175.

Rohlf, F. J., 2010. TPSDig2, version 2.16. URL `http://life.bio.sunysb.edu/morph/soft-dataacq.html`.

Sahli, H. F. and J. K. Conner, 2011. Testing for conflicting and nonadditive selection: floral adaptation to multiple pollinators through male and female fitness. Evolution 65:1457–1473.

Silvestro, D., A. Kostikova, G. Litsios, P. B. Pearman, and N. Salamin, 2015. Measurement errors should always be incorporated in phylogenetic comparative analysis. Methods Ecol Evol 9:340–346.

Skog, L. E., 2012. Gesneriaceae. Pp. 350–364, *in* P. Acevedo-Rodríguez and M. T. Strong, eds. Catalogue of seed plants of the west indies, *Smithsonian contributions to botany*, vol. 98. Smithsonian Institution Scholarly Press, Washington D.C.

Slater, G. J., 2013. Phylogenetic evidence for a shift in the mode of mammalian body size evolution at the Cretaceous-Palaeogene boundary. Methods Ecol Evol 4:734–744. URL `http://onlinelibrary.wiley.com/doi/10.1111/2041-210X.12084/abstract`.

Smith, S. D., 2010. Using phylogenetics to detect pollinator-mediated floral evolution. New Phytologist 188:354–363.

Stanton, M. L., A. A. Snow, and S. N. Handel, 1986. Floral evolution: attractiveness to pollinators increases male fitness. Science(Washington) 232:1625–1627.

Stebbins, G. L., 1970. Adaptive radiation of reproductive characteristics in angiosperms, I: Pollination mechanisms. Annual Review of Ecology and Systematics 1:307–326.

Sun, M., K. Gross, and F. P. Schiestl, 2014. Floral adaptation to local pollinator guilds in a terrestrial orchid. Ann Bot 113:289–300.

bioRxiv preprint doi: https://doi.org/10.1101/041533; this version posted October 13, 2017. The copyright holder for this preprint (which was not certified by peer review) is the author/funder, who has granted bioRxiv a license to display the preprint in perpetuity. It is made available under aCC-BY-NC 4.0 International license.

Thomas, G. H., R. P. Freckleton, and T. Székely, 2006. Comparative analyses of the influence of developmental mode on phenotypic diversification rates in shorebirds. Proceedings of the Royal Society of London B: Biological Sciences 273:1619–1624.

Thomas, G. H., S. Meiri, and A. B. Phillimore, 2009. Body size diversification in Anolis: novel environment and island effects. Evolution 63:2017–2030.

Uyeda, J. C., D. S. Caetano, and M. W. Pennell, 2015. Comparative analysis of principal components can be misleading. Syst Biol 64:677–689.

Valente, L. M., J. C. Manning, P. Goldblatt, P. Vargas, A. E. T.-L. R. Ashman, and E. M. A. McPeek, 2012. Did pollination shifts drive diversification in southern African Gladiolus? Evaluating the model of pollinator-driven speciation. The American Naturalist 180:83–98.

Waser, N. M., 1998. Pollination, angiosperm speciation, and the nature of species boundaries. Oikos 82:198–201.

Waser, N. M., L. Chittka, M. V. Price, N. M. Williams, and J. Ollerton, 1996. Generalization in pollination systems, and why it matters. Ecology 77:1043–1060.

Waser, N. M. and J. Ollerton, 2006. Plant-pollinator interactions: from specialization to generalization. University of Chicago Press.

Waser, N. M. and M. V. Price, 1981. Pollinator choice and stabilizing selection for flower color in *Delphinium nelsonii*. Evolution 35:376–390.

Whittall, J. B. and S. A. Hodges, 2007. Pollinator shifts drive increasingly long nectar spurs in columbine flowers. Nature 447:706–709.

Young, N. M., 2006. Function, ontogeny and canalization of shape variance in the primate scapula. Journal of Anatomy 209:623–636.

Yuan, Y.-W., K. J. Byers, and H. Bradshaw Jr., 2013. The genetic control of flower-pollinator specificity. Current Opinion in Plant Biology 16:422–428.

bioRxiv preprint doi: https://doi.org/10.1101/041533; this version posted October 13, 2017. The copyright holder for this preprint (which was not certified by peer review) is the author/funder, who has granted bioRxiv a license to display the preprint in perpetuity. It is made available under aCC-BY-NC 4.0 International license.

Table S1: Pollinator information for the species included in the study.

Species	Pollinator	Confirmed	Reference
Gesneria acaulis	hummingbird	yes	Marten-Rodriguez et al. 2009
Gesneria viridiflora subsp. acrochordonanthe	unknown	no	
Gesneria aspera	hummingbird	yes	Marten-Rodriguez et al. 2009
Gesneria bracteosa	unknown	no	
Gesneria citrina	hummingbird	yes	Marten-Rodriguez et al. 2008
Gesneria clarensis	unknown	no	
Gesneria cubensis	hummingbird	yes	Marten-Rodriguez et al. 2010
Gesneria cuneifolia	hummingbird	yes	Marten-Rodriguez et al. 2008
Gesneria duchartreoides	unknown	no	
Gesneria ekmanii	unknown	no	
Gesneria ferruginae	hummingbird	no	
Gesneria fruticosa	bat	yes	Marten-Rodriguez et al. 2009
Gesneria glandulosa	hummingbird	no	
Gesneria harrisii	hummingbird	no	
Gesneria humilis	moth	yes	Marten-Rodriguez et al. 2015
Gesneria lopezii	hummingbird	no	
Gesneria neglecta	bat	no	
Gesneria nipensis	hummingbird	no	
Gesneria pauciflora	hummingbird	no	
Gesneria pedicellaris	hummingbird	yes	Marten-Rodriguez et al. 2009
Gesneria pedunculosa	bat	yes	Marten-Rodriguez et al. 2008
Gesneria pulverulenta	hummingbird	yes	Marten-Rodriguez et al. 2009
Gesneria purpurascens	hummingbird	yes	Marten-Rodriguez et al. 2015
Gesneria quisqueyana	bat	yes	Marten-Rodriguez et al. 2009
Gesneria reticulata	hummingbird	yes	Marten-Rodriguez et al. 2015
Gesneria salicifolia	hummingbird	no	
Gesneria scabra	hummingbird	no	
Gesneria depressa	unknown	no	
Gesneria sintenisii	mixed-pollination	yes	Marten-Rodriguez et al. 2008
Gesneria sp	unknown	no	
Gesneria ventricosa	hummingbird	yes	Marten-Rodriguez et al. 2009
Gesneria viridiflora subsp. viridiflora	mixed-pollination	yes	Marten-Rodriguez et al. 2015
Gesneria yamuriensis	hummingbird	no	
Rhytidophyllum auriculatum	mixed-pollination	yes	Marten-Rodriguez et al. 2009
Rhytidophyllum berteroanum	hummingbird	yes	Marten-Rodriguez et al. 2009
Rhytidophyllum bicolor	unknown	no	
Rhytidophyllum bullatum	hummingbird	no	
Rhytidophyllum crenulatum	mixed-pollination	yes	Marten-Rodriguez et al. 2010
Rhytidophyllum earlei	hummingbird	no	
Rhytidophyllum exsertum	mixed-pollination	yes	Marten-Rodriguez et al. 2010
Rhytidophyllum grandiflorum	mixed-pollination	yes	Marten-Rodriguez et al. 2009
Rhytidophyllum intermedium	unknown	no	
Rhytidophyllum leucomallon	mixed-pollination	yes	Marten-Rodriguez et al. 2009
Rhytidophyllum lomensis	hummingbird	no	
Rhytidophyllum minus	mixed-pollination	yes	Marten-Rodriguez et al. 2015
Rhytidophyllum rupincola	hummingbird	yes	Marten-Rodriguez et al. 2010
Rhytidophyllum sp	unknown	no	
Rhytidophyllum tomentosum	mixed-pollination	yes	Marten-Rodriguez et al. 2010
Rhytidophyllum vernicosum	mixed-pollination	yes	Marten-Rodriguez et al. 2009
Bellonia spinosa	bee	yes	Marten-Rodriguez et al. 2008

bioRxiv preprint doi: https://doi.org/10.1101/041533; this version posted October 13, 2017. The copyright holder for this preprint (which was not certified by peer review) is the author/funder, who has granted bioRxiv a license to display the preprint in perpetuity. It is made available under aCC-BY-NC 4.0 International license.

Table S2: Information on the flower pictures included in the study.

FileName	CodeSpecies	Voucher
GES_acaulis_APR72R1_13.jpg	GES_acaulis	no_voucher
GES_acaulis_G877_G940_G1238_1.jpg	GES_acaulis	LHBH G877
GES_acaulis_JLC_11303_02.jpg	GES_acaulis	JLC 11303
GES_bracteosa_JLC_10567_53.jpg	GES_bracteosa	JLC 10567
GES_citrina_G888_Dec_1965_1.jpg	GES_citrina	LHBH G888
GES_citrina_JLC_10021_07.jpg	GES_citrina	JLC 10021
GES_clarensis_JLC_10488_117.jpg	GES_clarensis	JLC 10488
GES_cuneifolia_APR_72R9_1.jpg	GES_cuneifolia	no_voucher
GES_cuneifolia_Dunn_1.jpg	GES_cuneifolia	no_voucher
GES_cuneifolia_G763_BH_1973_1.jpg	GES_cuneifolia	LHBH G763
GES_cuneifolia_G784_G857_1.jpg	GES_cuneifolia	LHBH
GES_cuneifolia_G857_Puerto_Rico_Tapley_1965_2.jpg	GES_cuneifolia	LHBH G857
GES_cuneifolia_G869_G857_G763_1.jpg	GES_cuneifolia	LHBH
GES_cuneifolia_G869_Puerto_Rico_1963_Tapley_10_5_BH_4.jpg	GES_cuneifolia	LHBH G869
GES_cuneifolia_july_1980_1.jpg	GES_cuneifolia	no_voucher
GES_duchartreoides_JLC_12791_067.jpg	GES_duchartreoides	JLC 12791
GES_ferruginae_JLC_10627_083.jpg	GES_ferruginae	JLC 10627
GES_fruticosa_Cornell_G1035_01.jpg	GES_fruticosa	LHBH G1035
GES_fruticosa_Skog_01.jpg	GES_fruticosa	no_voucher
GES_glandulosa_JLC_12772_023.jpg	GES_glandulosa	JLC 12772
GES_harrisii_Jamaica_Guaco_Rock_3.jpg	GES_harrisii	no_voucher
GES_harrisii_Tapley_1964.jpg	GES_harrisii	no_voucher
GES_heterochroa_JLC_12800_061.jpg	GES_heterochroa	JLC 12800
GES_humilis_G1365_M_Stone_2.jpg	GES_humilis	LHBH G1365
GES_humilis_JLC_10040_06.jpg	GES_humilis	JLC 10040
GES_humilis_JLC_10472_11.jpg	GES_humilis	JLC 10472
GES_humilis_JLC_10574_14.jpg	GES_humilis	JLC 10574
GES_humilis_JLC_10584_01.jpg	GES_humilis	JLC 10584
GES_humilis_JLC_10589_25.jpg	GES_humilis	JLC 10589
GES_humilis_JLC_10624_04.jpg	GES_humilis	JLC 10624
GES_humilis_JLC_10630_05.jpg	GES_humilis	JLC 10630
GES_humilis_JLC_10633_13.jpg	GES_humilis	JLC 10633
GES_humilis_JLC_10634_10.jpg	GES_humilis	JLC 10634
GES_lopezii_Suarez_Cuba__Mayari_25.jpg	GES_lopezii	no_voucher
GES_neglecta_Cornell_G875_01.jpg	GES_neglecta	LHBH G875
GES_nipensis_JLC_10577_30.jpg	GES_nipensis	JLC 10577
GES_nipensis_JLC_10578_05.jpg	GES_nipensis	JLC 10578
GES_pauciflora_G769_1.jpg	GES_pauciflora	LHBH G769
GES_pauciflora_Gesneria_lemondrop_3.jpg	GES_pauciflora	no_voucher
GES_pedicellaris_domrep_talpey_1.jpg	GES_pedicellaris	no_voucher
GES_pedicellaris_G898_G883_G1231_1.jpg	GES_pedicellaris	LHBH
GES_pedicellaris_JLC_10635_04.jpg	GES_pedicellaris	JLC 10635
GES_pedicellaris_JLC_11328_13.jpg	GES_pedicellaris	JLC 11328
GES_pedicellaris_pauciflora_sacatilis_1.jpg	GES_pedicellaris	no_voucher
GES_pedunculosa_USBRG_1997_204_1.jpg	GES_pedunculosa	USBRG
GES_pedunculosa_USBRG_96_342_1.jpg	GES_pedunculosa	USBRG
GES_pulverulenta_G1034_1.jpg	GES_pulverulenta	LHBH G1034
GES_purpurascens_JLC_10564_124.jpg	GES_purpurascens	JLC 10564
GES_purpurascens_JLC_12769_096.jpg	GES_purpurascens	JLC 12769
GES_quisqueyana_APR_72R9_11.jpg	GES_quisqueyana	no_voucher
GES_reticulata_dominicanrepublic_talpey_1972_1.jpg	GES_reticulata	no_voucher
GES_reticulata_G784_3.jpg	GES_reticulata	LHBH G784
GES_reticulata_USBRG_1997_205_2.jpg	GES_reticulata	USBRG
GES_salicifolia_JLC_10566_79.jpg	GES_salicifolia	JLC 10566
GES_scabra_sphaerocarpa_G881_1.jpg	GES_scabra	LHBH G881
GES_scabra_sphaerocarpa_jamaica_talpey_1964_1.jpg	GES_scabra	no_voucher
GES_shaferi_JLC_12773_096.jpg	GES_depressa	JLC 12773
GES_shaferi_JLC_12786_012.jpg	GES_depressa	JLC 12786
GES_shaferi_JLC_12788_002.jpg	GES_depressa	JLC 12788
GES_ventricosa_dunn_4.jpg	GES_ventricosa	no_voucher
GES_ventricosa_G940_3.jpg	GES_ventricosa	LHBH G940
GES_ventricosa_JLC_6545_2.jpg	GES_ventricosa	JLC 6545
GES_viridiflora_JLC_10509_35.jpg	GES_viridiflora	JLC 10509
GES_viridiflora_JLC_10540_01.jpg	GES_viridiflora	JLC 10540
GES_viridiflora_JLC_10552_21.jpg	GES_viridiflora	JLC 10552

bioRxiv preprint doi: https://doi.org/10.1101/041533; this version posted October 13, 2017. The copyright holder for this preprint (which was not certified by peer review) is the author/funder, who has granted bioRxiv a license to display the preprint in perpetuity. It is made available under aCC-BY-NC 4.0 International license.

Table S2: Continued...

FileName	CodeSpecies	Voucher
GES_viridiflora_JLC_10554_20.jpg	GES_viridiflora	JLC 10554
GES_viridiflora_JLC_10555_29.jpg	GES_viridiflora	JLC 10555
GES_viridiflora_JLC_12797_14.jpg	GES_viridiflora	JLC 12797
GES_yamuriensis_JLC_10575_01.jpg	GES_yamuriensis	JLC 10575
RHY_auriculatum_USBRG_97_113_1.jpg	RHY_auriculatum	USBRG
RHY_berteroanum_77_227_4.jpg	RHY_berteroanum	no_voucher
RHY_berteroanum_G1398_G1257_G841_1.jpg	RHY_berteroanum	LHBH
RHY_berteroanum_JUL81W5_16.jpg	RHY_berteroanum	no_voucher
RHY_crenulatum_JLC_10042_38.jpg	RHY_crenulatum	JLC 10042
RHY_crenulatum_JLC_10580_10.jpg	RHY_crenulatum	JLC 10580
RHY_crenulatum_JLC_10582_02.jpg	RHY_crenulatum	JLC 10582
RHY_crenulatum_JLC_12803_09.jpg	RHY_crenulatum	JLC 12803
RHY_earlei_JLC_10458_02.jpg	RHY_earlei	JLC 10458
RHY_earlei_JLC_10486_19.jpg	RHY_earlei	JLC 10486
RHY_exsertum_JLC_10508_12.jpg	RHY_exsertum	JLC 10508
RHY_exsertum_JLC_10538_07.jpg	RHY_exsertum	JLC 10538
RHY_exsertum_JLC_10546_07.jpg	RHY_exsertum	JLC 10546
RHY_exsertum_JLC_10551_03.jpg	RHY_exsertum	JLC 10551
RHY_exsertum_JLC_10565_08.jpg	RHY_exsertum	JLC 10565
RHY_exsertum_JLC_10569_05.jpg	RHY_exsertum	JLC 10569
RHY_exsertum_JLC_10579_01.jpg	RHY_exsertum	JLC 10579
RHY_exsertum_JLC_10585_18.jpg	RHY_exsertum	JLC 10585
RHY_exsertum_JLC_12770_23.jpg	RHY_exsertum	JLC 12770
RHY_exsertum_JLC_12787_14.jpg	RHY_exsertum	JLC 12787
RHY_grandiflorum_APR72r9_8.jpg	RHY_grandiflorum	no_voucher
RHY_grandiflorum_cornell_1.jpg	RHY_grandiflorum	no_voucher
RHY_intermedium_JLC_10547_10.jpg	RHY_intermedium	JLC 10547
RHY_leucomallon_G1232_1.jpg	RHY_leucomallon	LHBH G1232
RHY_lomensis_JLC_10469_23.jpg	RHY_lomense	JLC 10469
RHY_lomensis_JLC_10470_24.jpg	RHY_lomense	JLC 10470
RHY_lomensis_JLC_10471_01.jpg	RHY_lomense	JLC 10471
RHY_minus_JLC_10500_34.jpg	RHY_minus	JLC 10500
RHY_rupincola_JLC_11308_18.jpg	RHY_rupincola	JLC 11308
RHY_rupincola_JLC_11957_36.jpg	RHY_rupincola	JLC 11957
RHY_tomentosum_apr72r1_11.jpg	RHY_tomentosum	no_voucher
RHY_tomentosum_jlc_10477_06.jpg	RHY_tomentosum	JLC 10477
GES_aspera_2014-011.jpg	GES_aspera	Lambert 2014-011
GES_cubensis_2014-008.jpg	GES_cubensis	Lambert 2014-008
GES_viridiflora_acrochordonanthe_2014-028.jpg	GES_acrochordonanthe	Lambert 2014-028
RHY_auriculatum_2014-014.jpg	RHY_auriculatum	Lambert 2014-014
RHY_auriculatum_2014-025.jpg	RHY_auriculatum	Lambert 2014-025
RHY_bicolor_2014-001.jpg	RHY_bicolor	Lambert 2014-001
RHY_bullatum_2014-016.jpg	RHY_bullatum	Lambert 2014-016
RHY_ekmanii_2014-020.jpg	GES_ekmanii	Lambert 2014-020
RHY_ekmanii_2014-024.jpg	GES_ekmanii	Lambert 2014-024
RHY_nov.sp._2014-010.jpg	GES_sp	Lambert 2014-010
RHY_sp_2014-022.jpg	RHY_sp	Lambert 2014-022
RHY_bicolor_2014-002.jpg	RHY_bicolor	Lambert 2014-002
GES_cuneifolia_JBM.jpg	GES_cuneifolia	JBM
GES_pedicellaris_JBM.jpg	GES_pedicellaris	JBM 932-1971
GES_ventricosa_JBM.jpg	GES_ventricosa	Léveillé-Bourret G4
RHY_auriculatum_JBM.jpg	RHY_auriculatum	JBM 937-1971
RHY_exsertum_JBM.jpg	RHY_exsertum	Léveillé-Bourret G1
RHY_rupincola_JBM.jpg	RHY_rupincola	JBM 113-1991
RHY_tomentosum_JBM.jpg	RHY_tomentosum	Léveillé-Bourret G2
RHY_vernicosum_JBM.jpg	RHY_vernicosum	Léveillé-Bourret G3
GES_sintenisii_JLC_13757_19.jpg	GES_sintenisii	JLC 13757
GES_acrochordonanthe_JLC_14467_090.jpg	GES_acrochordonanthe	JLC 14467
GES_acrochordonanthe_JLC_14522_045.jpg	GES_acrochordonanthe	JLC 14522
GES_glandulosa_JLC_14572_026.jpg	GES_glandulosa	JLC 14572
RHY_auriculatum_JLC_14319_34.jpg	RHY_auriculatum	JLC 14319
RHY_auriculatum_JLC_14387_37.jpg	RHY_auriculatum	JLC 14387
RHY_auriculatum_JLC_14434_01.jpg	RHY_auriculatum	JLC 14434
RHY_auriculatum_JLC_14499_10.jpg	RHY_auriculatum	JLC 14499
RHY_auriculatum_JLC_14523_028.jpg	RHY_auriculatum	JLC 14523

bioRxiv preprint doi: https://doi.org/10.1101/041533; this version posted October 13, 2017. The copyright holder for this preprint (which was not certified by peer review) is the author/funder, who has granted bioRxiv a license to display the preprint in perpetuity. It is made available under aCC-BY-NC 4.0 International license.

Table S2: Continued...

FileName	CodeSpecies	Voucher
RHY_bicolor_JLC_14321_109.jpg	RHY_bicolor	JLC 14321
RHY_bicolor_JLC_14364_05.jpg	RHY_bicolor	JLC 14364
RHY_bicolor_JLC_14493_07.jpg	RHY_bicolor	JLC 14493
RHY_leucomallon_JLC_14338_031.jpg	RHY_leucomallon	JLC 14338
RHY_leucomallon_JLC_14497_09.jpg	RHY_leucomallon	JLC 14497
RHY_leucomallon_JLC_14498_10.jpg	RHY_leucomallon	JLC 14498
RHY_nov.sp._JLC_14460_081.jpg	GES_sp	JLC 14460

Table S3: Voucher information for the specimens sequenced in the study.

Species	Collector	Collection number	Herbarium	Museum ID	F3H	uf3gt	chi	cycloidea	gapdh
Bellonia spinosa	Clark, J.	10573	UNA	MT-179392			sequenced	sequenced	sequenced
Bellonia spinosa	Léveillé-Bourret, É.	G8	MT	MT-184105	sequenced	sequenced	sequenced		
Gesneria acaulis	Clark, J.	11303	UNA	MT-179400	sequenced		sequenced	sequenced	sequenced
Gesneria acaulis	Martén-Rodriguez, S.	US-3479058-1188	US					GU323229	
Gesneria acrochordonanthe	Lambert, F	2014-027	MT	MT-194054			sequenced	sequenced	
Gesneria acrochordonanthe	Lambert, F	2014-028	MT	MT-194056	sequenced	sequenced	sequenced	sequenced	
Gesneria aspera	Lambert, F	2014-011	MT	MT-194032	sequenced		sequenced	sequenced	
Gesneria bracteosa	Clark, J.	10567	UNA	MT-179575	sequenced	sequenced	sequenced	sequenced	sequenced
Gesneria christii	Clark, J.	10025	UNA		sequenced		sequenced	sequenced	
Gesneria christii	Léveillé-Bourret, É.	G6	MT	MT-184103	sequenced	sequenced	sequenced	sequenced	sequenced
Gesneria christii	??	SI 94-507	??					AY363923	
Gesneria citrina	Clark, J.	10020	UNA		sequenced			sequenced	
Gesneria citrina	Martén-Rodriguez, S.	1248						GU323232	
Gesneria clarensis	Clark, J.	10488	UNA	MT-179401	sequenced	sequenced	sequenced	sequenced	sequenced
Gesneria cubensis	Lambert, F	2014-008	MT	MT-194027	sequenced		sequenced	sequenced	
Gesneria cubensis	Martén-Rodriguez, S.	JBSD-109650-1232	UNA					GU323234	
Gesneria cuneifolia	Martén-Rodriguez, S.	1247						GU323235	
Gesneria ekmanii	Lambert, F	2014-018	MT	MT-194044	sequenced	sequenced	sequenced	sequenced	
Gesneria ekmanii	Lambert, F	2014-020	MT	MT-194046	sequenced	sequenced	sequenced	sequenced	sequenced
Gesneria ekmanii	Lambert, F	2014-024	MT	MT-194050	sequenced		sequenced	sequenced	
Gesneria ferruginea	Clark, J.	10627	UNA	MT-179294		sequenced	sequenced	sequenced	sequenced
Gesneria fruticosa	Lambert, F	2014-012	MT	MT-194035	sequenced	sequenced	sequenced	sequenced	sequenced
Gesneria fruticosa	Martén-Rodriguez, S.	JBSD-109606-1227	UNA	MT-179391				GU323238	
Gesneria humilis	Clark, J.	10626	UNA	MT-179385	sequenced	sequenced	sequenced	sequenced	sequenced
Gesneria humilis	Clark, J.	10040	UNA	MT-179363	sequenced	sequenced	sequenced	sequenced	sequenced
Gesneria humilis	Clark, J.	10472	UNA		sequenced	sequenced	sequenced	sequenced	sequenced
Gesneria humilis	Clark, J.	10574	UNA				sequenced	sequenced	
Gesneria humilis	Chautems	1179						AY423156	
Gesneria nipensis	Clark, J.	10577	UNA	MT-179356	sequenced			sequenced	
Gesneria pedicellaris	Clark, J.	10635	UNA	MT-179354	sequenced	sequenced	sequenced	sequenced	
Gesneria pedicellaris	Martén-Rodriguez, S.	US-3498534-1229	US					GU323241	
Gesneria peduncolosa	Martén-Rodriguez, S.	1251						GU323242	
Gesneria pedunculosa	Clark, J.	10644	UNA	MT-179353	sequenced	sequenced	sequenced	sequenced	
Gesneria pulverulenta	Martén-Rodriguez, S.	US-3498527-1237	US					GU323243	
Gesneria pumila	Martén-Rodriguez, S.	1194	UNA	MT-179573				GU323244	
Gesneria purpurascens	Clark, J.	10564	UNA	MT-179351	sequenced	sequenced	sequenced	sequenced	sequenced
Gesneria quisqueyana	Martén-Rodriguez, S.	US-3498533-1230	US					GU323245	
Gesneria reticulata	Clark, J.	10558	UNA	MT-179347	sequenced	sequenced	sequenced	sequenced	
Gesneria reticulata	Martén-Rodriguez, S.	US-3498539-1221	US					GU323246	
Gesneria salicifolia	Clark, J.	10566	UNA	MT-179316	sequenced		sequenced	sequenced	sequenced
Gesneria depressa	Clark, J.	13070	UNA		sequenced			sequenced	
Gesneria sintenisii	Clark, J.	13757	UNA		sequenced	sequenced	sequenced	sequenced	
Gesneria sintenisii	Martén-Rodriguez, S.	1252		US-3594111				GU323250	
Gesneria ventricosa	Clark, J.	6545	UNA	MT-179344	sequenced			sequenced	sequenced
Gesneria ventricosa	Léveillé-Bourret, É.	G4	MT	MT-184101	sequenced	sequenced	sequenced	sequenced	sequenced
Gesneria ventricosa	Martén-Rodriguez, S.	1112A						GU323249	

bioRxiv preprint doi: https://doi.org/10.1101/041533; this version posted October 13, 2017. The copyright holder for this preprint (which was not certified by peer review) is the author/funder, who has granted bioRxiv a license to display the preprint in perpetuity. It is made available under aCC-BY-NC 4.0 International license.

Table S3: Continued...

Species	Collector	Collection number	Herbarium	Museum ID	F3H	uf3gt	chi	cycloidea	gapdh
Gesneria viridiflora	Clark, J.	10561	UNA	MT-179396				sequenced	
Gesneria viridiflora	Clark, J.	10524	UNA	MT-179386	sequenced	sequenced		sequenced	
Gesneria viridiflora	Clark, J.	10561	UNA	MT-179396		sequenced		sequenced	
Gesneria viridiflora	Clark, J.	10509	UNA					sequenced	
Gesneria viridiflora	Clark, J.	10540	UNA		sequenced			sequenced	
Gesneria viridiflora	Clark, J.	10041	UNA					sequenced	
Gesneria viridiflora	Hahn	440	??					AY626227	
Gesneria yumuriensis	Clark, J.	10575	UNA	MT-179275	sequenced	sequenced	sequenced	sequenced	sequenced
Henckelia malayana	Léveillé-Bourret, É.	G11	MT	MT-184108	sequenced		sequenced	sequenced	
Koehleria trinidad	no voucher		MT				sequenced	sequenced	
Rhytidophyllum auriculatum	Lambert, F	2014-014	MT	MT-194038	sequenced	sequenced	sequenced	sequenced	sequenced
Rhytidophyllum auriculatum	Lambert, F	2014-025	MT	MT-194051	sequenced	sequenced		sequenced	
Rhytidophyllum auriculatum	no voucher		MT		sequenced	sequenced		sequenced	sequenced
Rhytidophyllum auriculatum	Martén-Rodriguez, S.	US-3498538-1222	US					GU323253	
Rhytidophyllum berteroanum	Martén-Rodriguez, S.	JBSD-109605-1226						GU323254	
Rhytidophyllum bicolor	Lambert, F	2014-002	MT	MT-194022	sequenced	sequenced	sequenced	sequenced	sequenced
Rhytidophyllum bicolor	Lambert, F	2014-001	MT	MT-194020	sequenced	sequenced	sequenced	sequenced	sequenced
Rhytidophyllum bullatum	Lambert, F	2014-016	MT	MT-194041	sequenced	sequenced	sequenced	sequenced	
Rhytidophyllum crenulatum	Clark, J.	9531	UNA	MT-179273	sequenced	sequenced	sequenced	sequenced	sequenced
Rhytidophyllum crenulatum	Clark, J.	10580	UNA					GU323255	
Rhytidophyllum earlei	Clark, J.	10486	UNA	MT-179402	sequenced	sequenced	sequenced	sequenced	sequenced
Rhytidophyllum earlei	Clark, J.	10458	UNA	MT-179399	sequenced	sequenced	sequenced	sequenced	sequenced
Rhytidophyllum exsertum	Léveillé-Bourret, É.	G1	MT	MT-184098	sequenced	sequenced	sequenced	sequenced	sequenced
Rhytidophyllum exsertum	Clark, J.	10038	UNA	MT-179270	sequenced	sequenced	sequenced	sequenced	sequenced
Rhytidophyllum exsertum	Clark, J.	10585	UNA		sequenced		sequenced		
Rhytidophyllum exsertum	Skog, L.	1197-14						GU323256	
Rhytidophyllum grandiflorum	Martén-Rodriguez, S.	US-3498536-1224	US					GU323257	
Rhytidophyllum intermedium	Clark, J.	10549	UNA		sequenced	sequenced	sequenced	sequenced	sequenced
Rhytidophyllum leucomallon	Acevedo, P.	13966						GU323258	
Rhytidophyllum lomense	Clark, J.	10466	UNA	MT-179361	sequenced		sequenced	sequenced	sequenced
Rhytidophyllum lomense	Clark, J.	10469	UNA	MT-179358	sequenced	sequenced	sequenced	sequenced	sequenced
Rhytidophyllum minus	Clark, J.	10500	UNA	MT-179350	sequenced	sequenced	sequenced	sequenced	
Rhytidophyllum onacaensis	Carbono, E.	9085	UNA	MT-179308	sequenced	sequenced	sequenced	sequenced	sequenced
Rhytidophyllum rupincola	Clark, J.	11261	UNA	MT-179403	sequenced		sequenced	sequenced	sequenced
Rhytidophyllum rupincola	Clark, J.	11957	UNA	MT-179265	sequenced		sequenced	sequenced	sequenced
Rhytidophyllum rupincola	Léveillé-Bourret, É.	G5	MT	MT-184102	sequenced	sequenced		sequenced	sequenced
Rhytidophyllum rupincola	Martén-Rodriguez, S.	1253						GU323247	
Rhytidophyllum sp.	Lambert, F	2014-017	MT	MT-194043	sequenced		sequenced	sequenced	
Rhytidophyllum sp.	Lambert, F	2014-022	MT	MT-194049	sequenced		sequenced	sequenced	
Rhytidophyllum sp. nov 1	Lambert, F	2014-010	MT	MT-194030	sequenced	sequenced	sequenced	sequenced	sequenced
Rhytidophyllum sp. nov 1	Lambert, F	2014-009	MT	MT-194029	sequenced	sequenced	sequenced	sequenced	sequenced
Rhytidophyllum sp. nov 1	Lambert, F	2014-007	no voucher		sequenced	sequenced	sequenced	sequenced	sequenced
Rhytidophyllum tomentosum	Léveillé-Bourret, É.	G2	MT	MT-184099	sequenced	sequenced	sequenced	sequenced	sequenced
Rhytidophyllum tomentosum	Martén-Rodriguez, S.	US-3479065-1191						GU323260	
Rhytidophyllum tomentosum	??	SI77-235						AY363926	
Rhytidophyllum vernicosum	Léveillé-Bourret, É.	G3	MT	MT-184100	sequenced	sequenced	sequenced	sequenced	sequenced

bioRxiv preprint doi: https://doi.org/10.1101/041533; this version posted October 13, 2017. The copyright holder for this preprint (which was not certified by peer review) is the author/funder, who has granted bioRxiv a license to display the preprint in perpetuity. It is made available under aCC-BY-NC 4.0 International license.

Table S3: Continued...

Species	Collector	Collection number	Herbarium	Museum ID	F3H	uf3gt	chi	cycloidea	gapdh
Rhytidophyllum vernicosum	Martén-Rodriguez, S.	US-3498520-1246						GU323261	

bioRxiv preprint doi: https://doi.org/10.1101/041533; this version posted October 13, 2017. The copyright holder for this preprint (which was not certified by peer review) is the author/funder, who has granted bioRxiv a license to display the preprint in perpetuity. It is made available under aCC-BY-NC 4.0 International license.

bioRxiv preprint doi: https://doi.org/10.1101/041533; this version posted October 13, 2017. The copyright holder for this preprint (which was not certified by peer review) is the author/funder, who has granted bioRxiv a license to display the preprint in perpetuity. It is made available under aCC-BY-NC 4.0 International license.

Table S4: Primer information for the gene amplification.

Gene	Primers	Sequence (5' → 3')	Annealing temperature
CYCLOIDEA	gCYCf2	AAGGAGCTGGTGCAGGCTAAGA	54°C
	gCYCr2	GGGAGATTGCAGTTCAAATCCCTTGA	
GAPDH	GAPDHx1fb	TGCACTACTAACTGCCTTG	47°C
	GAPDHx4rb	GCTGGAAGMACTTTGCCAACAGC	
CHI	CHI1F	TCTGCATCGCTGTAGGTTCC	59°C
	CHI1R	GACATGTCTTGCCACCCAACT	
UF3GT	UF3GT1F	TGCCAAAATCCACCGCTGTGT	51°C
	UF3GT1R	TGCAACTGAGGTGCCCAGGA	
F3H	F3H2f	ACGGAGGCCTACAGCGAGCA	56°C
	F3H2R	CCTGCAACCCACCCACCTGA	

Note: PCR reactions included 1 × buffer, 1 mM $MgSO_4$, 1 U DreamTaq (Thermoscientific), 0.4 μM of each primer, 0.2 μM of each dNTPs, 1% PVP (M.W. 40,000), 50 μg BSA and ca. 30 ng of DNA.

bioRxiv preprint doi: https://doi.org/10.1101/041533; this version posted October 13, 2017. The copyright holder for this preprint (which was not certified by peer review) is the author/funder, who has granted bioRxiv a license to display the preprint in perpetuity. It is made available under aCC-BY-NC 4.0 International license.

Table S5: Number of transitions between the different pollination strategies according to the stochastic mapping when performed on species with confirmed and inferred pollination strategies. The median values obtained from the character simulations over the posterior distribution of species tree is reported as well as 95% credible intervals. Ancestral state are in rows.

	bat	bee	hummingbird	mixed-pollination	moth
bat	–	0.25 [0.19, 0.22]	3.74 [3.07, 4.40]	3.70 [3.06, 4.30]	0.22 [0.14, 0.34]
bee	0.06 [0.02, 0.10]	–	0.05 [0.02, 0.10]	0.08 [0.02, 0.14]	0.03 [0.02, 0.05]
hummingbird	3.32 [2.55, 3.88]	0.43 [0.37, 0.51]	–	2.48 [2.00, 2.96]	0.63 [0.44, 0.78]
mixed-pollination	4.47 [3.82, 5.17]	0.28 [0.20, 0.37]	6.53 [5.54, 7.15]	–	0.25 [0.14, 0.33]
moth	0.03 [0.02, 0.11]	0.06 [0.04, 0.10]	0.04 [0.01, 0.07]	0.04 [0.02, 0.07]	–

bioRxiv preprint doi: https://doi.org/10.1101/041533; this version posted October 13, 2017. The copyright holder for this preprint (which was not certified by peer review) is the author/funder, who has granted bioRxiv a license to display the preprint in perpetuity. It is made available under aCC-BY-NC-4.0 International license.

Table S6: Parameter values of the univariate evolutionary models fitted on the first three principal components of the morphospace when species with confirmed and inferred pollinators were included in the analyses. Mean values from the posterior distribution of species trees are given for the AICc weights, whereas median values are given for the parameter estimates. Numbers in brackets indicate the 25% and the 75% quantiles. The best model for each component is in bold. The θ parameter indicate the global or regime means for the BM-type and OUBM-type models, whereas it indicates the stationary optimum trait for the OU-type models. $station_{hum}$ and $station_{mix}$ are the stationary distributions of the hummingbird and mixed-pollination strategies.

PC1

Models	p	AICc weight	θ_{hum}	θ_{mix}	σ^2_{hum}	σ^2_{mix}	$station_{hum}$	$station_{mix}$
BM1	2	0 [0,0]	0.042 [0.033,0.05]	0.042 [0.033,0.05]	0.105 [0.077,0.163]	0.105 [0.077,0.163]	–	–
BMV	3	0 [0,0]	0.097 [0.033,0.137]	0.097 [0.033,0.137]	0.028 [0.016,0.13]	0.151 [0.059,0.285]	–	–
BM1m	**3**	**0.38 [0.03,0.69]**	**0.154 [0.148,0.162]**	**-0.129 [-0.139,-0.118]**	**0.015 [0.012,0.019]**	**0.015 [0.012,0.019]**	–	–
BMVm	4	0.16 [0.03,0.24]	0.153 [0.143,0.16]	-0.132 [-0.142,-0.122]	0.019 [0.013,0.025]	0.011 [0.009,0.014]	–	–
OU1	3	0 [0,0]	0.031 [0.021,0.042]	0.031 [0.021,0.042]	0.207 [0.137,0.477]	0.207 [0.137,0.477]	0.033 [0.031,0.034]	0.033 [0.031,0.034]
OUM	4	0.46 [0.03,0.95]	0.169 [0.165,0.172]	-0.159 [-0.159,-0.158]	3.122 [0.916,17.092]	3.122 [0.916,17.092]	0.005 [0.005,0.005]	0.005 [0.005,0.005]
OUMV	5	0 [0,0]	0.214 [0.192,0.23]	-0.163 [-0.192,-0.075]	15.291 [4.636,43.424]	24.445 [10.766,50.789]	2.25 [1.027,5.547]	4.309 [1.556,7.299]
OUMA	5	0 [0,0]	0.218 [0.198,0.247]	-0.159 [-0.196,-0.08]	21.291 [12.123,39.902]	21.291 [12.123,39.902]	3.587 [2.64,4.543]	3.587 [2.64,4.543]
OUMVA	6	0 [0,0]	0.214 [0.19,0.231]	-0.162 [-0.195,-0.096]	17.889 [4.882,42.186]	24.258 [10.321,52.843]	2.414 [1.005,4.92]	4.403 [1.848,7.136]
OUBMi	4	0 [0,0]	0.123 [0.096,0.146]	0.123 [0.096,0.146]	1.797 [0.063,43.782]	0.038 [0.018,0.119]	0.014 [0.007,0.017]	–
BMOUi	4	0 [0,0]	-0.053 [-0.074,-0.03]	-0.053 [-0.074,-0.03]	0.033 [0.021,0.066]	2.751 [0.442,33.744]	–	0.019 [0.013,0.023]
OUBM	3	0 [0,0]	0.15 [0.118,0.177]	0.15 [0.118,0.177]	0.171 [0.118,0.285]	0.171 [0.118,0.285]	0.005 [0.004,0.007]	–
BMOU	3	0 [0,0]	-0.091 [-0.119,-0.036]	-0.091 [-0.119,-0.036]	0.188 [0.122,0.336]	0.188 [0.122,0.336]	–	0.008 [0.006,0.011]

PC2

Models	p	AICc weight	θ_{hum}	θ_{mix}	σ^2_{hum}	σ^2_{mix}	$station_{hum}$	$station_{mix}$
BM1	2	0 [0,0]	-0.033 [-0.036,-0.03]	-0.033 [-0.036,-0.03]	0.021 [0.016,0.035]	0.021 [0.016,0.035]	–	–
BMV	3	0 [0,0]	-0.032 [-0.037,-0.027]	-0.032 [-0.037,-0.027]	0.029 [0.02,0.055]	0.009 [0.007,0.012]	–	–
BM1m	3	0 [0,0]	-0.018 [-0.024,-0.012]	-0.057 [-0.064,-0.051]	0.019 [0.014,0.033]	0.019 [0.014,0.033]	–	–
BMVm	4	0 [0,0]	-0.012 [-0.02,0]	-0.05 [-0.059,-0.039]	0.028 [0.019,0.052]	0.007 [0.005,0.009]	–	–
OU1	**3**	**0.53 [0.45,0.65]**	**-0.028 [-0.03,-0.026]**	**-0.028 [-0.03,-0.026]**	**0.223 [0.075,0.99]**	**0.223 [0.075,0.99]**	**0.003 [0.003,0.003]**	**0.003 [0.003,0.003]**
OUM	4	0.26 [0.23,0.32]	-0.04 [-0.043,-0.034]	-0.017 [-0.019,-0.014]	0.169 [0.075,0.662]	0.169 [0.075,0.662]	0.003 [0.003,0.003]	0.003 [0.003,0.003]
OUMV	5	0.05 [0.01,0.07]	-0.049 [-0.055,-0.038]	-0.02 [-0.027,-0.012]	9.117 [5.89,13.777]	3.756 [2.774,5.29]	1.132 [0.884,1.613]	0.482 [0.408,0.568]
OUMA	5	0.02 [0,0.03]	-0.049 [-0.056,-0.039]	-0.016 [-0.026,-0.008]	6.422 [4.583,9.904]	6.422 [4.583,9.904]	0.796 [0.7,0.974]	0.796 [0.7,0.974]
OUMVA	6	0.01 [0,0.02]	-0.049 [-0.056,-0.038]	-0.02 [-0.028,-0.012]	9.189 [5.72,13.364]	3.717 [2.825,5.463]	1.117 [0.865,1.458]	0.486 [0.411,0.583]
OUBMi	4	0.1 [0.01,0.06]	-0.041 [-0.047,-0.035]	-0.041 [-0.047,-0.035]	0.289 [0.11,1.407]	0.006 [0.004,0.009]	0.003 [0.003,0.003]	–
BMOUi	4	0.01 [0,0]	-0.023 [-0.033,-0.017]	-0.023 [-0.033,-0.017]	0.028 [0.019,0.049]	0.045 [0.023,0.225]	–	0.002 [0.002,0.002]
OUBM	3	0 [0,0]	-0.045 [-0.051,-0.037]	-0.045 [-0.051,-0.037]	0.032 [0.021,0.05]	0.032 [0.021,0.05]	0.003 [0.003,0.004]	–
BMOU	3	0 [0,0]	-0.024 [-0.033,-0.017]	-0.024 [-0.033,-0.017]	0.03 [0.021,0.051]	0.03 [0.021,0.051]	–	0.002 [0.002,0.002]

PC3

Models	p	AICc weight	θ_{hum}	θ_{mix}	σ^2_{hum}	σ^2_{mix}	$station_{hum}$	$station_{mix}$
BM1	2	0.02 [0,0.03]	0.018 [0.015,0.019]	0.018 [0.015,0.019]	0.004 [0.004,0.005]	0.004 [0.004,0.005]	–	–
BMV	3	0.01 [0,0.01]	0.017 [0.015,0.019]	0.017 [0.015,0.019]	0.005 [0.005,0.007]	0.003 [0.003,0.005]	–	–
BM1m	3	0.12 [0.03,0.16]	0.031 [0.028,0.034]	-0.004 [-0.009,-0.001]	0.004 [0.003,0.004]	0.004 [0.003,0.004]	–	–
BMVm	4	0.05 [0.02,0.08]	0.035 [0.03,0.039]	-0.001 [-0.004,0.003]	0.005 [0.004,0.006]	0.002 [0.002,0.003]	–	–
OU1	**3**	**0.3 [0.13,0.45]**	**0.015 [0.014,0.016]**	**0.015 [0.014,0.016]**	**0.019 [0.013,0.107]**	**0.019 [0.013,0.107]**	**0.002 [0.002,0.002]**	**0.002 [0.002,0.002]**
OUM	4	0.1 [0.03,0.15]	0.018 [0.016,0.021]	0.01 [0.009,0.013]	0.02 [0.013,0.209]	0.02 [0.013,0.209]	0.002 [0.001,0.002]	0.002 [0.001,0.002]
OUMV	5	0.12 [0.03,0.16]	0.022 [0.017,0.029]	0.01 [0.005,0.017]	2.865 [2.249,3.919]	0.854 [0.702,1.063]	0.449 [0.394,0.524]	0.146 [0.118,0.17]
OUMA	5	0.03 [0.01,0.04]	0.022 [0.016,0.026]	0.01 [0.005,0.018]	1.359 [1.089,1.744]	1.359 [1.089,1.744]	0.275 [0.249,0.301]	0.275 [0.249,0.301]
OUMVA	6	0.02 [0.01,0.03]	0.023 [0.019,0.029]	0.01 [0.006,0.017]	2.135 [1.616,2.726]	0.733 [0.569,0.944]	0.399 [0.348,0.467]	0.148 [0.118,0.177]
OUBMi	4	0.01 [0,0.01]	0.017 [0.014,0.02]	0.017 [0.014,0.02]	0.015 [0.01,0.027]	0.003 [0.002,0.004]	0.002 [0.002,0.003]	–
BMOUi	4	0.13 [0.02,0.16]	0.016 [0.014,0.017]	0.016 [0.014,0.017]	0.004 [0.004,0.005]	0.048 [0.02,0.229]	–	0.001 [0.001,0.001]
OUBM	3	0.01 [0,0.01]	0.018 [0.015,0.021]	0.018 [0.015,0.021]	0.005 [0.004,0.007]	0.005 [0.004,0.007]	0.003 [0.002,0.007]	–
BMOU	3	0.08 [0.01,0.1]	0.015 [0.012,0.017]	0.015 [0.012,0.017]	0.006 [0.006,0.008]	0.006 [0.006,0.008]	–	0.001 [0.001,0.001]

bioRxiv preprint doi: https://doi.org/10.1101/041533; this version posted October 13, 2017. The copyright holder for this preprint (which was not certified by peer review) is the author/funder, who has granted bioRxiv a license to display the preprint in perpetuity. It is made available under aCC-BY-NC 4.0 International license.

Table S7: Matrix of stationary variance estimates obtained with the OUM multivariate model, averaged over the posterior distribution of species trees with only species with confirmed pollination strategies. Median values are reported and numbers in brackets indicate the 25% and the 75% quantiles.

	PC1	PC2	PC3
PC1	0.0058 [0.0055, 0.0062]		
PC2	0.00063 [0.00053, 0.00081]	0.0029 [0.0029, 0.0030]	
PC3	-0.0010 [-0.0013, -0.00070]	-0.00058 [-0.00064, -0.00053]	0.0020 [0.0018, 0.0022]

bioRxiv preprint doi: https://doi.org/10.1101/041533; this version posted October 13, 2017. The copyright holder for this preprint (which was not certified by peer review) is the author/funder, who has granted bioRxiv a license to display the preprint in perpetuity. It is made available under aCC-BY-NC 4.0 International license.

Table S8: Model performance with the multivariate evolutionary models fitted on the first three principal components of the morphospace when all species were included in the analyses, including those with inferred pollinator strategies. The mean values obtained from the posterior distribution of species trees are given; numbers in brackets indicate the 25% and the 75% quantiles. The best model is in bold.

models	logLik	param	AICc weight
BM1	108.11 [98.93,120.48]	9	0 [0,0]
BMV	119.69 [112.64,128.69]	15	0 [0,0]
BM1m	140.93 [133.11,152.03]	12	0 [0,0.01]
BMVm	147.9 [140.66,156.66]	18	0 [0,0]
OU1	136.62 [132.59,140.57]	15	0 [0,0]
OUM	**164.32 [162.02,166.75]**	**18**	**1 [0.99,1]**
OUBM	123.15 [117.04,131.4]	15	0 [0,0]
BMOU	121.65 [115.22,130.89]	15	0 [0,0]
OUBMr	142.66 [140.17,146.98]	21	0 [0,0]
BMOUr	130.75 [123.82,139.6]	21	0 [0,0]

bioRxiv preprint doi: https://doi.org/10.1101/041533; this version posted October 13, 2017. The copyright holder for this preprint (which was not certified by peer review) is the author/funder, who has granted bioRxiv a license to display the preprint in perpetuity. It is made available under aCC-BY-NC 4.0 International license.

Table S9: Model parameters for the multivariate OUM model, which was the model that received the highest $AICc$ weight (Table S8), when all species are included in the analysis. The mean values obtained from the posterior distribution of species trees are given; numbers in brackets indicate the 25% and the 75% quantiles.

parameters	PC1	PC2	PC3
θ_{hum}	0.173 [0.169,0.177]	-0.042 [-0.052,-0.037]	0.015 [0.008,0.019]
θ_mix	-0.16 [-0.162,-0.158]	-0.017 [-0.018,-0.014]	0.011 [0.009,0.016]
σ^2	3.132 [0.987,10.306]	0.7 [0.232,2.32]	0.091 [0.018,0.372]
phylogenetic halftime	0.001 [0,0.003]	0.013 [0.004,0.039]	0.122 [0.079,0.21]
stationary variance	0.004 [0.004,0.005]	0.003 [0,0]	0.001 [-0.001,0]

bioRxiv preprint doi: https://doi.org/10.1101/041533; this version posted October 13, 2017. The copyright holder for this preprint (which was not certified by peer review) is the author/funder, who has granted bioRxiv a license to display the preprint in perpetuity. It is made available under aCC-BY-NC 4.0 International license.

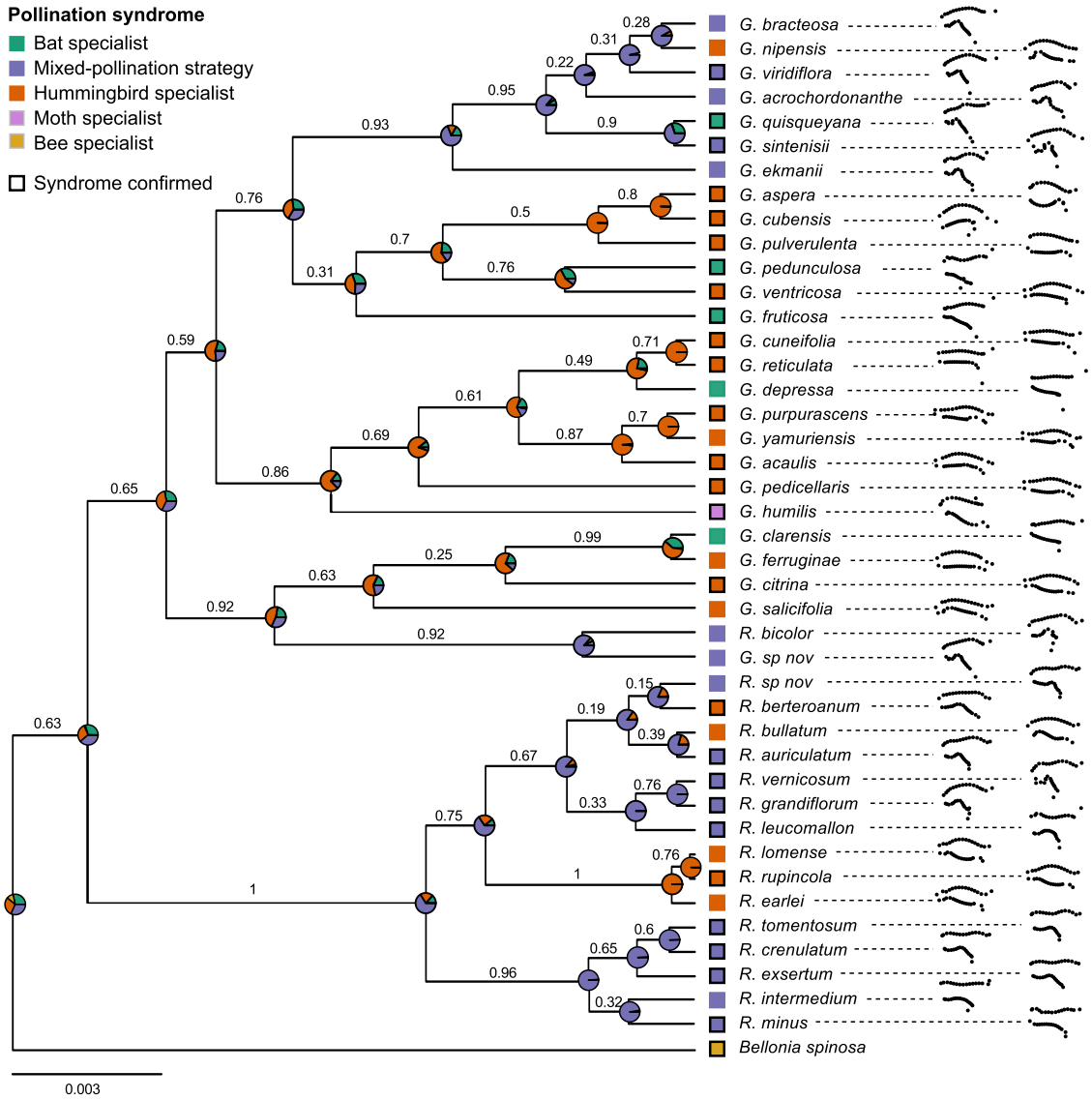

Figure S1: Species phylogeny showing mean corolla shapes (after Procrustes analysis). Pollination strategies are shown with those that have been confirmed indicated by a black contour. Pie charts represent the joint probability of each state at nodes as estimated by stochastic mapping from all species, that is including species with inferred pollinators. Clade posterior probabilities are shown above branches. Outgroup taxa are not shown.

bioRxiv preprint doi: https://doi.org/10.1101/041533; this version posted October 13, 2017. The copyright holder for this preprint (which was not certified by peer review) is the author/funder, who has granted bioRxiv a license to display the preprint in perpetuity. It is made available under aCC-BY-NC 4.0 International license.

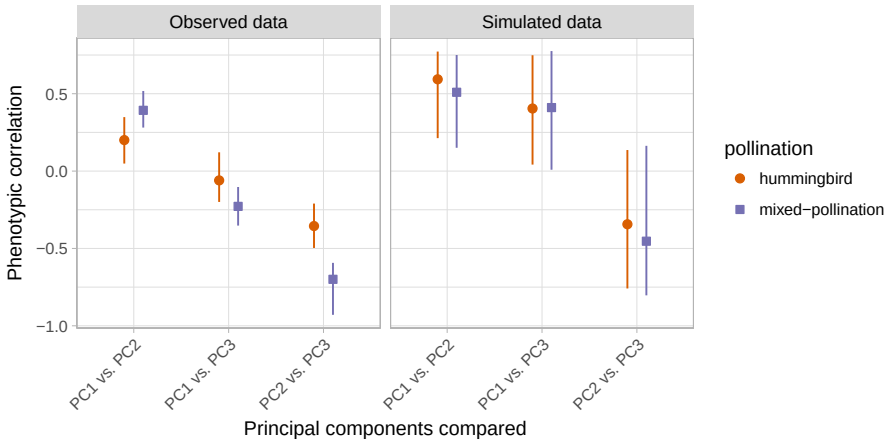

Figure S2: Graphical representation of the evolutionary correlations (i.e., standardized evolutionary rates matrices) obtained with the BMVm multivariate model when all species were included in the analysis, for the observed data (left panel) and for data simulated under the best fitting model (OUM; right panel). Symbols represent the median correlation and the lines the 25% and 75% quantiles for both hummingbirds and mixed-pollination strategies. No artifactual differences are detected between the two groups when fitting models on traits simulated with the OUM model and thus with a common evolutionary covariance (right panel, see text).